Review article

Bone char as a green sorbent for removing health threatening fluoride from drinking water

Susan S.A. Alkurdi[a,b], Raed A. Al-Juboori[a,c], Jochen Bundschuh[a,d,*], Ihsan Hamawand[e]

[a] School of Civil Engineering and Surveying, Faculty of Health, Engineering and Sciences, University of Southern Queensland, West Street, Toowoomba, 4350, Queensland, Australia
[b] Northern Technical University, Engineering Technical College, Kirkuk, Iraq
[c] School of Science, Engineering and Information Technology, Federation University Australia, University Drive, Mt Helen, VIC 3350
[d] UNESCO Chair on Groundwater Arsenic within the 2030 Agenda for Sustainable Development, University of Southern Queensland, West Street, Toowoomba, 4350, Queensland, Australia
[e] Research and Engineering Services, Toowoomba, QLD, 4350, Australia

ARTICLE INFO

ABSTRACT

Millions of people around the world suffer from or prone to health problems caused by high concentration of fluoride in drinking water sources. One of the environmentally friendly and cost-effective ways for removing fluoride is the use of bone char. In this review, the structural properties and binding affinity of fluoride ions from different water sources was critically discussed. The effect of experimental conditions on enhancing the adsorption capacity of fluoride ions using bone char samples was addressed. It appears that surface properties, and conditions of the bone char production such as temperature and residence time play an important role in designing the optimal fluoride removal process. The optimum temperature for fluoride removal seems to be in the range of 500–700 °C and a residence time of 2 h. Applying various equilibrium adsorption isotherms for understanding fluoride adsorption mechanism was presented. The effect of bone char modification with different elements were discussed and recommendations for a further increase in the removal efficiency was proposed. Cost of bone char production and large-scale treatment systems were also discussed based on information available from scientific and commercial sources. Challenges with existing domestic defluoridation designs were highlighted and suggestions for new conceptual designs were provided.

1. Introduction

Fluorine is the most reactive electronegative element. Fluorine's leaching and dissolution into groundwater and thermal gases occurs due to the processes of weathering and water circulation within soil layers and rocks. It also has a high affinity to acquire electrons and form negative fluoride ions (F$^-$). Thus, fluoride forms complexes with several cations, which constitutes about (0.6–0.9%) of the Earth's crust. Its concentration is about 1 mg/L in sea water, 0.5 mg/L in lakes and rivers (Fawell et al., 2006) and (1–35 mg/L) in groundwater (Tripathy et al., 2006). The concentration of fluoride in groundwater resources depends on the geographical location and is largely associated with the presence of nearby volcanic activities and fumarolic gases. Some of the high fluoride concentrations belts extend on lands along the East African Rift, between Turkey and China, USA, South America, Japan, Australia etc. (Maheshwari, 2006). There are a wide variety of fluoride minerals

present in the soil texture such as fluorspar, rock phosphate, apatite, cryolite, mica, sellaite, phlogopite, topaz, etc. (Elango and Jagadeshan, 2018). In addition, soil conditions such as alkalinity, high levels of aluminum and low concentrations of calcium and magnesium oxides are important factors that increase F$^-$ leaching into groundwater (Padhi and Muralidharan, 2012). On the other hand, anthropogenic sources of F$^-$ in the environment are due to two main sources. Firstly, the release and mobilization of fluoride of a geological origin into the environment from some processes such as coal combustion, and secondly from the improper discharge of waste products by various industries, including nickel, steel, copper and aluminum smelting; and the industrial manufacture of masonry, ceramics, semiconductors, phosphate fertilizers and glass (Cai et al., 2017; Rasool et al., 2017; Tovar-Gómez et al., 2013; Waghmare et al., 2015) are also responsible for fluoride availability in water resources.

Fluoride is categorized as an essential substance as it contributes in
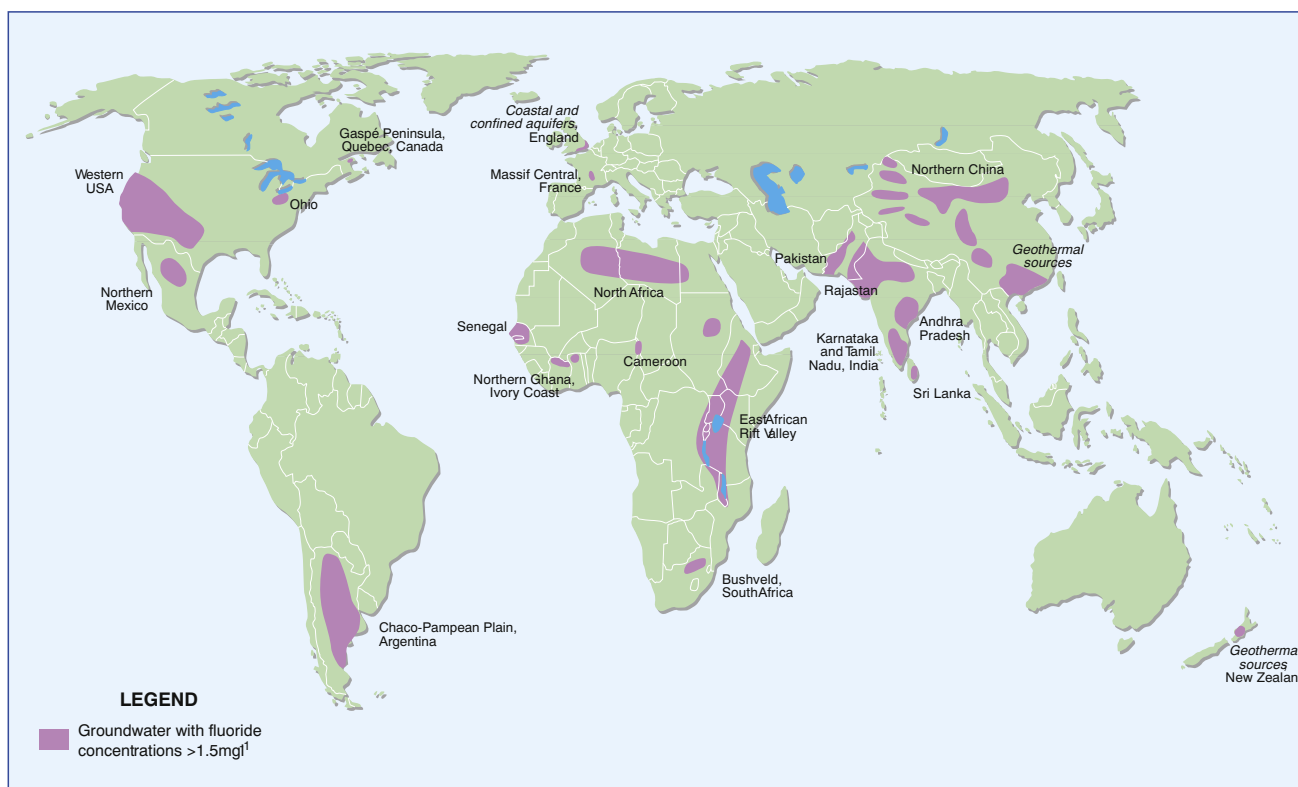

Fig. 1. Countries with high level of fluoride in groundwater. Reproduced with the permission of the British Geological Survey ©UKRI, All rights Reserved, Permit Number: CP19/030 (Edmunds and Smedley, 2013).

the development and the maintenance of dental health. However, some health hazards have been associated with the ingestion of high concentrations of fluoride via drinking water. The absorption of fluoride ions, its distribution to the tissues and bio-accumulation in bones and teeth results in many well-recognized adverse effects. According to a UNICEF report, tens of millions of people have endemic fluorosis in 25 countries globally; especially countries in volcanic areas (Petrone et al., 2013). Fluorosis emanating from excess presence of fluoride in drinking water is a serious issue worldwide as it was reported that > 35 countries worldwide have excess of fluoride in drinking water (Ayoob et al., 2008) (see Fig. 1). Most of the countries highlighted in Fig. 1 are situated in regions with from sediments of marine origin, volcanic rocks and granitic and gneissic rocks such as those in the geographical line extending from Jordan valley to Eastern Africa and central Asia trough the Mediterranean region (Fawell et al., 2006). Other health effects related to consuming high fluoride concentrations (higher than 1.0 mg/ L) are effects on the immune and human reproductive systems, children's neurodevelopment, kidney and gastrointestinal tract health (Harrison, 2005). Furthermore, it was reported that fluoride can form strong bonds with other toxic metals such as aluminum and lead, altering the toxicity of the substance when digested (Jackson et al., 2002). Therefore, much research effort was focused on developing technologies for fluoride removal from aqueous media in order to reduce its concentrations to levels below 1.5 mg/L, which is the current WHO and Australian guidelines limit for F^- in drinking water (Fawell et al., 2006).

Some of the methods used to remove fluoride from water include co-precipitation (Chigondo et al., 2018), precipitation-coagulation (Ye et al., 2018), electrocoagulation (Changmai et al., 2018; Zhu et al., 2007), adsorption (Mourabet et al., 2015; Wang et al., 2013), ion exchange (Meenakshi et al., 2008) and membrane processes (Jeihanipour et al., 2018; Lhassani et al., 2001; Pan et al., 2018), or a combination of these technologies (Wei et al., 2015; Zhang and Jia, 2018). However, these methods have issues including high operating cost, waste

production, strict pH and other experimental conditions and the use of toxic chemicals, all of which are limiting factors for their use in water defluoridation. Of all these methods, adsorption has been reported to be the most promising method for the removal of fluoride from water due to the high removal efficiency, superior adsorption rate, ease of operation and the availability of a wide range of adsorbents. Among many different types of adsorbent materials including activated carbon (Raychoudhury et al., 2017), cellulosic materials (Nagaraj et al., 2017), zeolites (Abaei et al., 2017; Lai et al., 2018), aluminum (Karmakar et al., 2017), nanomaterials (Maity et al., 2018; Rostamia et al., 2017), biochars (Dewage et al., 2018; Roy, 2018; Wang et al., 2018) and bone char (Delgadillo-Velasco et al., 2017; Ismail and AbdelKareem, 2015; Medellin-Castillo et al., 2007). Bone char has gained considerable attention owing to its low cost, ease of preparation and biocompatibility (Nunes-Pereira et al., 2018).

This work aims to review bone char's removal capacity of fluoride from water, with the main focus of providing a comprehensive overview of bone char preparation, modification techniques and their respective fluoride removal efficiencies. The effect of several parameters, such as pH, initial concentration, bone char dosage rate and temperature, on fluoride uptake will be discussed. These factors are of great significance, as any change in these parameters may significantly alter the fluoride removal efficiency of the adsorbent. Therefore, a general knowledge of the effect of these parameters is critical in designing the appropriate drinking water treatment facilities. Cost of bone char production, successful industrial bone char treatment attempts and design aspects were also discussed in this study.

2. Bone char production and characteristics

Globally, millions of tons of bone waste are produced annually due to the meat industry. According to the Organisation for Economic Co-operation and Development (OECD) reports (OECD, 2018), it is expected that there will be an increase of 40 million metric tons in meat
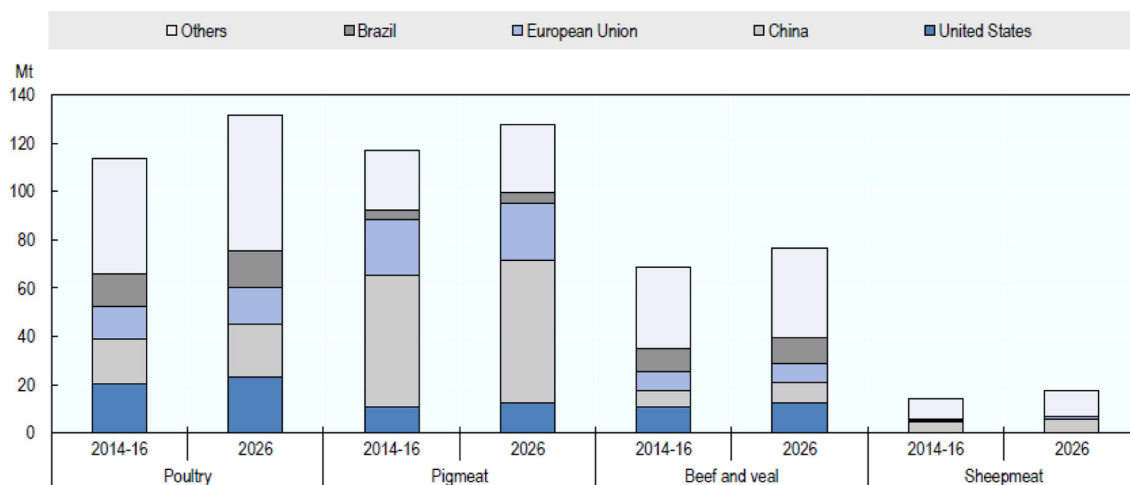
Fig. 2. Meat production by type and country (OECD, 2018).

production within the next ten years, including 13% in poultry, 10% in pig meat and > 21% in sheep meat. As a consequence, there will be a significant increase in meat and bone meal waste produced globally. Fig. 2 shows meat production statistics between 2014 and 2016, and the expected increase in meat production by 2026 in some countries. It is important to highlight here that in spite of the expected increase in waste bone, its application for defluoridation can be hampered by the customs and religious beliefs of people (e.g. char originated from cow bones is not acceptable by Hindus and similarly pigs bone char is not acceptable by Muslims). Thus, educating communities is essential for applying bone char for defluoridation.

The similarity in the bone structure of poultry and red meat species (Field et al., 1974) makes harnessing bone waste for fluoride removal a topic of interest globally as some countries may consume a certain type of meat more than others as shown in Fig. 2. However, it is important to note that the bone structure of a certain animal species may differ with age and parity (Field et al., 1974; Keene et al., 2004). The bone structure can also differ from one part to another in the animal body. Interestingly, it was found that calcium to nitrogen ratio increased in bones with age for red meat species and poultry (Field et al., 1974) and this may serve well fluoride removal given the capacity of calcium in binding with fluoride (Meenakshi et al., 2008).

Thermal treatment of animal bones is one of the methods used for safe disposal of bone waste through incineration, to ensure destruction of any pathogens. This process is mainly carried out through co-incineration in cement kilns, or by stand-alone incineration plants. However, attention to energy recovery from waste and environmental benefits of the process have attracted the attention of many researchers in order to provide a clean energy source as an alternative to fossil fuel (Usón et al., 2013). Bone char is considered as one of the adsorbents with low negative impact on the environment and human health as oppose to other waste-based adsorbents such as aluminum oxide amended wood char and activated alumina (Yami et al., 2015). The ability of regenerating bone char is an attractive trait and it makes the char a promising green sorbent for water defluoridation. However, the lifespan of bone char can only be estimated based on several factors such as F^- initial concentration, the capacity of the plant and the removal capacity of the bone char (Naliaka, 2016). The regeneration aspect of bone char will be explained in detail in Section 6.

Combustion in a limited oxygen environment through pyrolysis and gasification has been adopted in recent years for the purpose of energy generation from bone waste and use of the solid product (bone char) for environmental remediation and soil amendment applications. For maximizing the energy recovery of bone char production, gasification would be the preferred method as the produced syngas can be used as fuel to power gasification reactor. Limited number of studies have

investigated this approach and were successful in producing syngas and bone char (Soni et al., 2009, 2011). However, the focus of these studies was on increasing the amount of gases produced with high heating values and bone char was only a by-product. To have a balanced approach perhaps a multi-factor optimization of gasification process taking into account energy consumed, gas produced, heating value of the gases and bone char produced should be conducted to identify the optimal operating parameters for this process.

Appetites are minerals that are widely distributed in igneous rocks. Bioapatite is the biological form of inorganic calcium phosphate salts (Liu et al., 2013) with a general formula of $Ca_5(PO_4,CO_3)_3(OH,F,Cl,CO_3)$ (Skinner and Jahren, 2004). Bone apatite is a carbonate apatite with 6–9% carbonate composition in the apatite structure (Ishikawa et al., 2018). However, bone sintering process leads to change the form of apatite minerals in bones to hydroxyapatite (HAP). Figueiredo et al. (2010) examined the effect of calcination temperature on the apatite form using bovine bones reporting that bone char samples produced up to 600 °C were made of carbonate apatite, while raising the temperature up to 900 and 1200 °C resulted in the formation of HAP. Thus, the amount and the form of apatite content of a bone char is related to the charring temperature and thermal treatment period.

Bone char has long been used as an absorbent for decolorization in the sugar industry (Kader et al., 1996). It has high pollutant removal efficiency attributed to its principal characteristics represented by the textural properties of bone char and the hydroxyapatite content. Bone char is made of 70–76% hydroxyapatite (HAP), 7–9% calcium carbonate and 9–11% amorphous carbon (Mendoza-Castillo et al., 2015; Reynel-Avila et al., 2016; Rojas-Mayorga et al., 2015a). However, in a different scenario, bone char was reported to be made of 80–90% HAP and 10% amorphous carbon (Lambert and Graham, 1989). Hydroxyapatite $(Ca_{10}(PO_4)_6(OH)_2)$, which is an inorganic material, was reported as an advantageous material due to its applications in electrochemistry (Goodman et al., 2013), as a catalyst (Mohamed and Baeissa, 2013; Xie et al., 2013), and for environmental remediation (Li et al., 2018; Oladipo and Gazi, 2017; Thanh et al., 2017).

Carbonization of crushed animal bones includes heat treatment of a carbonaceous precursor at temperatures mainly higher than 500 °C and below 700 °C (Cheung et al., 2001b), in a limited oxygen environment to pyrolyze the raw material into a porous material (Cheung et al., 2001a). In such a process, partial evolution of the volatile matter from the carbonaceous precursor will take place. Further increase in pyrolyzation temperature exceeding 700 °C will alter the physical properties of the bone char. Rojas-Mayorga et al. (2015a) reported that after raising the temperature from 650 °C up to 1000 °C, a gradual color changing of the bone to white was noticed, which indicates the

Table 1

The effect of charring temperature and heating rate on the bone char surface properties and fluoride uptake (residence time = 2 h).

Factors		Effect			Purging gas	Reference
Temperature (°C)	Heating rate (°C/min)	BET surface area (m^2/g)	Total pore volume (cm^3/g)	Fluoride uptake (mg/g)		
650	5	–	–	6.7	N$_2$ gas	Rojas-Mayorga et al. (2013)
	10	118	0.24	6.51		
700	5	–	–	6.96		
	10	110	0.233	7.32		
800	5	–	–	6.67		
	10	–	0.224	6.71		
900	5	–	–	2.99		
	10	–	–	3.03		
1000	5	–	–	1.34		
	10	–	–	1.24		
650	5	–	–	5.52 ± 0.08	CO$_2$ gas	Rojas-Mayorga et al. (2015c)
	10	62	0.2	5.33 ± 0.14		
700	5	–	–	5.78 ± 0.05		
	10	69	0.3	5.92 ± 0.03		
800	5	–	–	0.74 ± 0.13		
	10	9	0.16	0.81 ± 0.02		
900	5	–	–	0		
	10	4	0.04	0		
1000	5	–	–	0		
	10	2	0.02	0		

complete elimination of the organic matter in the bone char structure. Kawasaki et al. (2009) reported that high pyrolysis temperature results in the degradation of the functional groups and lowering the efficiency of water defluoridation.

Calcination temperature has a great effect on the surface area and pore volume of bone char. For instance, raising calcination temperature from 650 °C to 700 °C under a CO$_2$ atmosphere resulted in an increase of the specific surface area from 62 to 69 m^2/g and the total pore volume from 0.2 to 0.23 cm^3/g of cow bone char, respectively (Rojas-Mayorga et al., 2015a). However, further increase in the temperature to 1000 °C reduced the surface area and the pore volume of the material to 2 m^2/g and 0.02 cm^3/g; and altered the color of the bone char to white. The latter was used as an indication for fluoride removal capacity of the bone char, which was reduced from 5.92 to 0 mg/g after raising pyrolysis temperature from 700 to 900 °C. Tables 1 and 2 show the effect of charring temperature at different residence times and heating rates on the BET surface area of bone char.

Pyrolyzing conditions are critical factors that affect the textural and chemical composition of bone char. Residence time and heating rate are essential factors to control the quality of the bone char produced at different temperatures. Generally, based on the bone source, pyrolysis between 500 and 700 °C seems to be a critical pyrolysis temperature for bone char used for water defluoridation (taking into account the limitations related to the residence time and the rate of temperature). Lowering the temperature below 500 °C will result in adding more organic matter to the treated water due to the incomplete removal of organic matter in the bone structure. On the other hand, raising the charring temperature will result in the dihydroxylation of the HAP. Table 1 presents a summary of the outcome of previous studies on the effect of temperature and heating rate on bone char properties.

Purging gas used during pyrolysis is an important factor in controlling bone char quality for different environmental applications. Rojas-Mayorga et al. (2015a) examined the effect of pyrolyzed cattle bone in CO$_2$ and N$_2$ atmospheres for the purpose of fluoride removal from water. While both samples were exhibiting a mesoporous structure, bone char samples pyrolyzed in an N$_2$ environment had higher specific surface area and total pore volume of 85 m^2/g, 0.24 cm^3/g than those pyrolyzed at the same temperature, residence time and heating rate with CO$_2$ as a purging gas (Tables 1 and 2). Although the removal of F$^-$ on the bone char surface was due to their exchange with OH

functional groups (i.e. chemical reaction), the increase in the surface area and the pore volume was vital in providing a higher contact possibility of F$^-$ with the active functional groups.

Bone source and calcination temperature may have an effect on the FTIR signals received from bone chars, but the main components of bone char are well defined. The inorganic components (calcium and phosphate) of any bone char are reported to be almost the same but with different fractions (Tovar-Gómez et al., 2013). FTIR spectra of bone char pyrolyzed at different temperatures are always those of typical hydroxyapatite but with varying peaks intensity (Fig. 3). Tovar-Gómez et al. (2013) examined two commercial bone chars, namely BCM from Carbones Mexicanos (Mexico) and BCB (Brimac 216) from Brimac Carbon Services (United Kingdom), for their fluoride uptake capacity using both bone char dispersion in the medium (henceforth referred to as batch) and column experiments. The study suggested that the higher removal capacity of the BCM than BCB samples related to their chemical composition. The higher oxygen and hydrogen content (consequently, hydroxyl groups) for the BCM samples were the reason behind its higher adsorption capacity of fluoride as illustrated in Eq. (1):

$$Ca_{10}(PO_4)_6OH + 2F^- \rightarrow Ca_{10}(PO_4)_6F_2 + 2OH^- \tag{1}$$
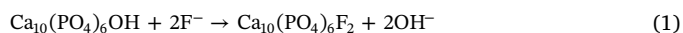
2.1. Removal mechanism

As mentioned previously, the effectiveness of bone char for fluoride removal is due its hydroxyapatite content. The removal mechanisms of fluoride on bone char is illustrated in Fig. 4. As it can be seen from this figure that there are three removal mechanisms; ion exchange, precipitation and electrostatic interaction (Sternitzke et al., 2012) or a combination of these mechanisms.

The ion exchange is the main mechanism of F$^-$ due to the high affinity of F$^-$ to substitute the hydroxide group in the structure of the HAP to form the fluorapatite (Ca$_{10}$(PO$_4$)$_6$F$_2$). However, the electrostatic interaction between the bone char surface and the F$^-$ plays an important role in the removal process. This mechanism is affected by the changes in the pH of the solution, in which it controls the isoelectric point of the bone char surface and hence affects its electrical attraction to entities in proximity to it. At pH levels below the point of zero charge (this will be discussed further in Section 3.3), the surface of the bone char is positively charged and this will increase the affinity of the

Table 2
The effect of charring temperature and residence time on the bone char surface properties and fluoride uptake (heating rate = 10 °C/h).

Factors		Effect			Purging gas	Reference
Temperature (°C)	Residence time (h)	BET Surface area (m^2/g)	Total pore volume (cm^3/g)	Fluoride uptake (mg/g)		
200	1	2	–	2.55[a]	Limited O_2	Terasaka et al. (2014)
400	1	114	–	2.85[a]		
600	1	73	–	1.65[a]		
650	2	118	0.24	6.51	N_2 gas	Rojas-Mayorga et al. (2013)
	4		–	6.63		
700	2	110	0.233	7.32		
	4		–	7.16		
800	2	96	0.224	6.71		
	4	–	–	6.57		
900	2	–	–	3.03		
	4	–	–	3.01		
1000	2	–	–	1.24		
	4	–	–	1.25		
650	2	62	0.2	5.33 ± 0.014	CO_2 gas	Rojas-Mayorga et al. (2015c)
	4	–	–	5.45 ± 0.06		
700	2	69	0.3	5.92 ± 0.03		
	4	–	–	5.72 ± 0.09		
800	2	9	0.16	0.81 ± 0.02		
	4	–	–	0.67 ± 0.08		
900	2	4	0.04	0		
	4	–	–	0		
1000	2	2	0.02	0		
	4	–	–	0		
400	1	98.626	0.291	–	Limited O_2	Patel et al. (2015)
	2	114.149	0.294	–		
	3	92.402	0.315	–		
450	1	98.138	0.305	–		
	2	83.948	0.302	–		
500	1	78.172	0.294	–		
	2	69.788	0.321	–		
600	1	57.939	0.293	–		
	2	50.37	0.305	–		

[a] Data were calculated from the figures and the data available in the article.
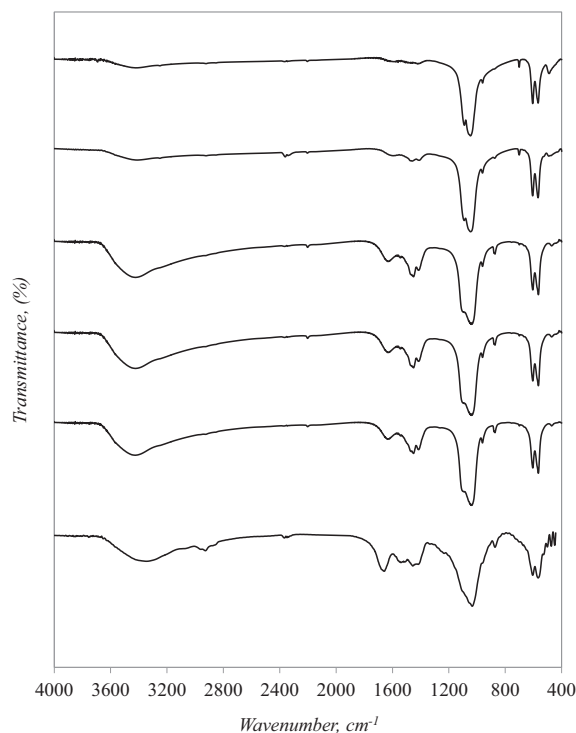
Fig. 3. FTIR spectrum for raw bone and bone char samples pyrolyzed at different temperatures: (a) raw bone, (b) 650 °C, (c) 700 °C, (d) 800 °C, (e) 900 °C and (f) 1000 °C (Rojas-Mayorga et al., 2013).

negatively charged F^- ions to adsorb onto the char. The formation of fluoride precipitants on the surface of the bone char takes part with high F^- concentrations (Herath et al., 2018) or in the case of metal coated bone char with cations such as Al^{3+}, Fe^{3+} etc. In this case, precipitants such as CaF_2, AlF_3 or FeF_3 will be formed on the char surface (Nigri et al., 2017b; Rojas-Mayorga et al., 2015b; Zhu et al., 2011). So, the prominence of the mechanisms in the removal process depends on the characteristics of the water being treated (e.g. pH and fluoride concentration).

2.2. Bone char modification

Suitable activation methods can lead to improve the adsorption capacity of carbonaceous materials via increasing the surface area, pore volume or providing a diversity of pore sizes to the adsorbent; or altering surface functional groups in a way that increases the selectivity of the adsorbent toward specific contaminants. However, bone char examinations after different modification methods indicate that there are no significant increments in the surface area (Delgadillo-Velasco et al., 2017). Thus, considerations regarding improvement in adsorption capacity of bone chars are mostly related to altering the functional groups on the surface. Table 3 summarizes the effect of different modification methods and experimental conditions on the removal capacity of F^- on bone char samples. Zúñiga-Muro et al. (2017) doped two different cerium precursors (Ce^{3+} and Ce^{4+}) onto cattle bone char for enhancing fluoride removal from water. The composite was reported to be beneficial for its stability for different pH ranges and potential antibacterial properties. The results showed a significant increase in the removal capacity of F^- on the Ce^{4+} modified bone char from 5.47 to 13.6 mg/g at pH 7. The acidic characteristic of the cerium
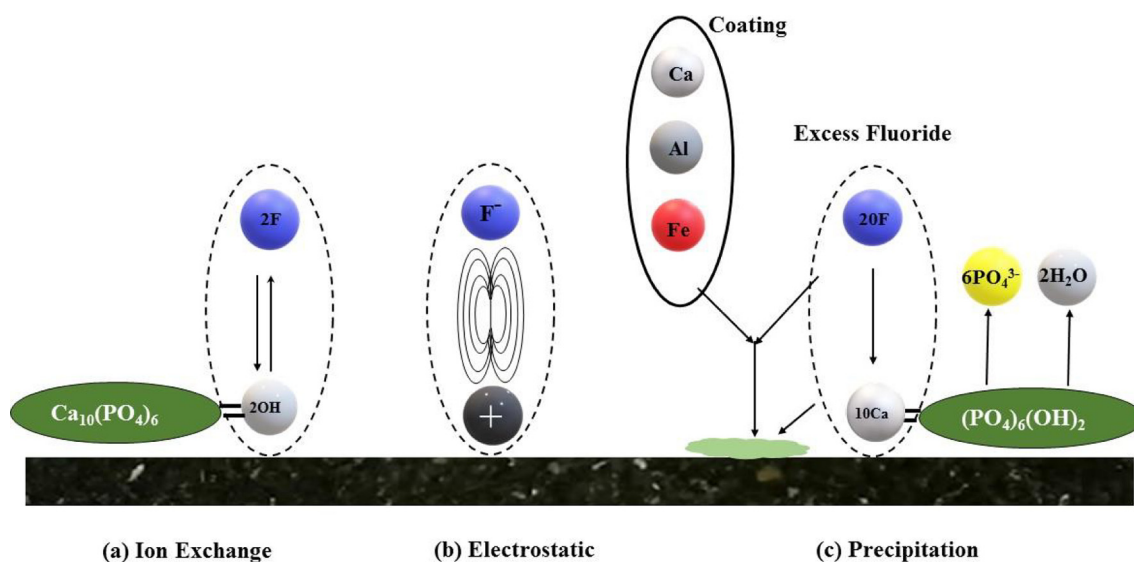
Fig. 4. Mechanisms of fluoride removal on bone char.

solution resulted in the dissolution of hydroxyapatite and release of phosphate to solution, which reacted with the cerium precursors and subsequently precipitated on the adsorbent surface. Then, an ion exchange between the calcium content of the HAP and the cerium precursor was the main mechanism behind the removal of fluoride ions on the modified bone char. On the other hand, the Ce^{3+} doped bone's ability to remove fluoride from water was lower than that of the pristine bone char in some cases due to the dissolution of Ce^{+3} in the washing stages. As a consequence, the adsorbent lost the active calcium and cerium sites after being washed out from the char surface at pH 7.

Zhu et al. (2011) used cattle bone char after modifying it with different aluminum salts ($AlCl_3$, $AlNO_3$, $NaAlO_2$, $Al_2(SO_4)_3$) to remove fluoride from water. The maximum removal onto $AlCl_3$ modified bone char was 97% at pH 7, for a 10 mg/L F^- initial concentration, 10 g/L adsorbent dosage and 72 h contact time. Similarly, bone char modification using $AlCl_3.6H_2O$ resulted in a maximum removal capacity of 6.8 mg F^-/g bone char from water (Nigri et al., 2017b), while bone char pre-treatment with $Ca(OH)_2$, $FeCl_3$, $CaCl_2$ and $MgCl_2$ were reported to be less effective for fluoride removal (4.4, 1.56, 5.1 and 4.2 mg/g, respectively). Rojas-Mayorga et al. (2015c) examined the effect of doping aluminum sulfate onto bovine bone char (pyrolyzed at 700 °C) for fluoride removal from water using packed bed micro-columns. The bed capacity to remove fluoride was 3.3–18.5 mg/g at pH 7, F^- feed concentration 10–100 mg/L and feed rate of 0.18–0.36 L/h. The Al doped bone char removed about 500% fluoride more than the commercial bone char samples used by Tovar-Gómez et al. (2013), but with different column dimensions and experimental conditions. Bone char coated with aluminum sulfate was examined for its effectiveness by comparing it to another 3 metal salts for fluoride removal from water in a batch reactor (Rojas-Mayorga et al., 2015b). Different metals ($Al(OH)_xF_y$, Fe_xF_y, and CaF_2) doped onto the bone char surface contributed significantly to the improvement of the removal efficiency. The maximum adsorption capacity achieved was 31 mg/g using aluminum sulfate doped bone char at pH 7 and 100 mg/L initial F^- concentration. In contrast, the maximum removal on the unmodified bone char was only 7.32 mg/g (Rojas-Mayorga et al., 2013), which means that there was a significant improvement in the removal capacity of fluoride ions from solution after modification. Chatterjee et al. (2018) used aluminum sulfate in combination with calcium oxide to chemically treat carbonized bone meal (a mixture of chicken and cattle bones) for fluoride removal at high initial concentrations (20–1000 mg/L). The new modified bone char resulted in enhancing the removal capacity of fluoride from 14 to 150 mg/g. Delgadillo-Velasco et al. (2017) studied

the effect of doping colloidal Ag onto commercial bone char samples at different temperatures (300, 400 and 500 °C) for fluoride removal from water. The results showed that the thermal treatment at 400 °C was the most appropriate temperature for bonding Ag colloids to the bone char surface. However, thermal treatment of bone char at the same temperature showed that the increase in fluoride uptake on the bone char with and without Ag colloids are almost the same (about 20% more than the untreated bone char), but the antibacterial effect of doping Ag was a new characteristic for the composite. The thermally treated commercial bone char resulted in removal of 1.65 mg/g fluoride from solution, owing to the irreversible loss of lattice water and its effect on the lattice dimension of the hydroxyapatite in the temperature range 200–400 °C. Another explanation for this improvement in F^- removal was due to the dehydration of the hydroxyapatite after the thermal treatment of the bone char, which was considered to be equivalent to the effect of charring bone samples at 850 °C in which the dislocation of lattice will occur (Liao et al., 1999). Eq. 2 shows the OH group loss due to thermal treatment of hydroxyapatite (Rojas-Mayorga et al., 2013):

$$2Ca_5(PO_4)_3OH \rightarrow Ca_{10}(PO_4)_6(OH)_{(2-2x)}O_x\square_x + xH_2O \qquad (2)$$
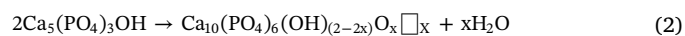
where $\square$ represents a vacancy. It is clear from the observations on bone char modification that such a practice can improve the char absorptivity of F^-, however the extent of improvement varies from one element to another. Fluoride ions in solution will be highly attracted to multivalent metal ions (such as aluminum, iron, zinc etc.) owing to their small size and high electronegativity (Tchomgui-Kamga et al., 2010). Thus, the difference in the electronegativity of the used multivalent metal ions are the main reason behind their higher removal capacity of some metal ions. For instance, the higher difference in electronegativity between fluoride and Al(III) than that with Fe(III) resulted in higher removal capacity of fluoride ions from solution with Al(III) coated bone char.

2.3. Bone char treatment cost for industrial scale systems

Bone char was reported as an adsorbent for water defluoridation since 1937 (Dahi, 2016), while the first full-scale defluoridation plant using bone char was constructed in South Dakota in 1953 followed by several others distributed over different locations in California. Groundwater that was treated in these plants contained F^- concentrations of 9–12 mg/L (State of South Carolina Department of Health and Environmental Control Water Supply Division, 1980). In 1988, household scale bone char filters, with incorporation of charcoal, were

Table 3
Removal capacity and experimental conditions for fluoride removal on bone char.

Bone Char	F⁻ removal mg/g	pH	Initial concentration mg/L	Charring temperature °C	Surface area m²/g	Pore volume cm³/g	Contact time	Isotherm model	References
Cattle BC	11.9	3.0	1–20	-	104	-	2–3 d	Langmuir and Freundlich	Medellin-Castillo et al. (2007)
	2.71	7.0							
Commercial BC	7.74	5.0	1–20	-	104	-		Langmuir, Freundlich and Radke-Prausnitz	Medellin-Castillo et al. (2014)
HAP	11.1	7.0		-	62.9	-			
Fish BC	2.15 ± 0.121			300 °C	24.2 ± 2.19	-	1 h	Langmuir and Freundlich	Brunson and Sabatini (2009)
Fish BC	5.01 ± 0.015			400 °C	98.7 ± 0.3				
Fish BC	4.85 ± 0.025			500 °C	111 ± 1.63				
Fish BC	3.89 ± 0.230			600 °C	112 ± 2.29				
Cow BC	5.96 ± 0.322			400 °C	110 ± 1.35				
Commercial BC	2.72		2–200	-	-	-	20 h	Langmuir and Freundlich	Sani et al. (2016)
0.1 M HCL washed cow BC	6.2	7.7 ± 0.2	10	700–800	138.8	0.308	50 h	Langmuir and Freundlich	Nigri et al. (2017a)
Al-impregnated cow bone char	6.3	6.4 ± 0.3							
Ox BC	0.64	8.4–11.3	0.26–1.05 mmol/L	580	-	-	24 h	-	Larsen et al. (1993)
Commercial BC		4.9–9.2	0–20		-	-	3 h	Freundlich	Abe et al. (2004)
Al modified cattle BC	0.97	7	2–20		-	-	72 h	-	Zhu et al. (2007)
Commercial BC		7	1–20	-	104	0.3	2d	Langmuir, Freundlich and Prausnitz-Radke	Leyva-Ramos et al. (2010)
Cattle BC modified with Ce⁺⁴	13.6	7	10–300	700 under N₂	-	-	840 min	Langmuir, Freundlich and Sips	Zúñiga-Muro et al. (2017)
BC for synthesized water	0.056	7.6	1–6	500–600	-	-	10 h	Langmuir and Freundlich	Smittakorn et al. (2010)
BC for field groundwater	0.157		3.5						
Commercial BC	0.8	-	5–50	-	65	0.098	72 h	-	Delgadillo-Velasco et al. (2017)
Ag doped thermally treated BC	1.28			400	59	0.109			
Cow BC	7.32	7	10–50	700	110	0.233	24 h	Langmuir and Freundlich	Rojas-Mayorga et al. (2013)
Cow BC under CO₂ environment	5.92 ± 0.03	7	5–80	700	69	0.23	24 h	-	Rojas-Mayorga et al. (2015c)
Cow BC under NO₂ environment	7.32				85	0.24			
Al doped cow BC	3.3–18.5	7	10–100	700	85	-	-	-	Rojas-Mayorga et al. (2015a)
Al sulfate doped BC	31	7	10–100	700	-	-	-	Langmuir	Rojas-Mayorga et al. (2015b)
Carbonized bone meal (CBM)	14	6.1	20–1000	550	58	0.01	24 h	Langmuir, Freundlich and Dubinin-Radushkevich	Chatterjee et al. (2018)
Chemically treated CBM	150				110	0.3			
Cuttlefish BC	0.283	4.5	2.5–10	-	0.07 ± 0.002	-	60 min	-	Nasr et al. (2011)
Carbones Mexicanos BC	2.26–5.0	7	9–40	-	104	-	1.5–3.0 min	Langmuir, Freundlich and Sips	Tovar-Gómez et al. (2013)
Brimac 216 BC	0.47–2.47				129	-			

used for water defluoridation in Thailand (Phantumvanit et al., 1988). Bone char filters were also used in many areas affected by high F⁻ concentrations in water sources in Tanzania and Kenya. One of the most efficient plants were constructed in Nakuru city to serve the city and the surrounding areas through the work of four different types of filters with different capacities ranging from 10 to 2,000,000 L/day (Näslund and Snell, 2005). With regards to the removal capacity of large scale bone char systems, a study conducted by Yami et al. (2015) showed that 496 kg bone char/100 m³ water is required for reducing F⁻ concentration from 10 to 1.5 mg/L. Generally, the main cost elements of water treatment facilities are capital cost and operation and maintenance cost. Hansen et al. (1979) estimated the cost of constructing a water defluoridation system to range from ~ $55,380 USD to ~ $168,620 USD (about $192,008.41 to $584,623.66 USD in 2019 after adding the inflation, respectively) for a plant capacity of 2.57 and 126 m³/h, respectively. Thereby the operation cost was reported to be ~ $9180 USD to ~ $25,010 USD (about $31,828.05 and $86,721.36 USD in 2019 after adding the inflation, respectively) for the same plants.

It seems that there is limited scientific detailed reports on the cost estimation for bone char production on a large scale, and what is available is confined to limited commercial reports. This can be attributed to the fact that the cost of the production is subjective and depends on various factors that are location specific in nature such as capital cost, availability and cost of labor, raw materials etc. Arrenberg (2010) reported that the cost of producing five tons of bone char (using mainly, goat, camel, cattle and sheep bones from different suppliers) by CDN's company was estimated to be $1609.87 USD (about $1858.35 in 2019 after adding the inflation). The cost of production included the energy consumption, cost related to materials and chemicals, and labor salaries, which represents about 20.6, 58.6 and 20.8% of the total cost, respectively. The recent cost figures for bone char production can be inferred from the available market sale prices as advertised by commercial companies. Surely the cost of production would be less than the sale prices or have been compensated by the energy gain from other product of the bone pyrolysis (i.e. useful gases produced from gasification). The recent advertised price of 25 kg of bone char produced from cow bones at 800 °C is $299 USD (~ $12 USD/kg) (Bulk Bone Char® Promolife Inc), while the same amount of cattle bone char can cost about $1.2 USD based on Alibaba online company price (only big bulk orders of 20 metric tons at least) (Alibaba.com). This shows that bone char cost can be very low if it is produced on a large scale.

3. Effect of adsorption parameters

3.1. Equilibrium contact time

Adsorption equilibrium is the period of time in which adsorption and desorption processes reach equilibrium. In other words, the amount of the adsorbed material from the solution is equal to the amount of the desorbed material from the adsorbent (Çeçen and Aktas, 2011). Equilibria data is essential for assessing adsorption process, characterizing an adsorbent, examining the removal capacity of the adsorbate and the respective rate of adsorption for their application in industrial processes (Leyva-Ramos et al., 2010).

Adsorption of fluoride on bone char has been shown to follow a general trend of adsorption in which the removal capacity is fast at the beginning of the reaction owing to the availability of large numbers of active sites on the surface. Then, adsorption rate slows down gradually until the equilibrium is reached. Leyva-Ramos et al. (2010) studied the rate of fluoride adsorption on bone char in terms of diffusional and kinetic models reporting that the rate of fluoride removal is mainly controlled by the pore volume. In contrast, Abe et al. (2004) reported that the removal of fluoride ions from solution is due to the ion exchange between the phosphate dissociated from the calcium phosphate composition of bone char at low pH levels and fluoride ions in solution.

Fluoride adsorption rates for different bone chars were reported to reach equilibrium in the range of 20 h to 5 days, which is a long period when considering fluoride removal for industrial applications. Zúñiga-Muro et al. (2017) determined the removal rate of fluoride ions onto cow bone char, based on the results achieved using a pseudo second order equation, to range between 2.3×10^{-3} and 4.89×10^{-3} g/mg min. This result is comparable to the results reported by Rojas-Mayorga et al. (2013) (from 8.02×10^{-4} to 2.94×10^{-3} g/mg min) and to a lesser extent Rojas-Mayorga et al. (2015b) (from 1.71×10^{-5} to 3.11×10^{-5} g/mg min) for an equilibrium time of 24 h to remove fluoride using cow bone char and Al doped bone char, respectively, using the same kinetic model, but with different experimental conditions.

Chatterjee et al. (2018) reported a very rapid reduction in fluoride concentration in solution from 10 to 0.13 mg/L in 1 h (about 98.7%) using aluminum sulfate and calcium oxide thermally treated bone meal. Equilibrium reached after 24 h with a removal efficiency of 99.6%. The difference in the column dimensions, inter-bead voids, flow rate and hydrodynamic effects are the key factors to control the removal capacity of a contaminate. Issues related to the non-uniform void ratio through column filtration will affect the efficiency of the columns. Generally, increasing the number of beds in a column provides more active sites for contaminants to settle and a higher break through curve, which are due to the increase in the mass transfer zone. However, increasing the number of beds will also be accompanied by the use of longer columns and thus providing channeling issues and accordingly reducing the efficiency of filtration.

3.2. Effect of initial concentration and adsorbent dose

It is essential to examine the effect of changing the solute initial concentration in an adsorption process to find out the optimum conditions for substance uptake. Up to a certain limit, the removal percentage (removal efficiency) of fluoride ions on bone char increases with increasing fluoride initial concentration. Then, no more adsorption will take place owing to the limited vacant sites available for adsorbate particles. This may be explained based on the Fickian definition, which suggest that the gradient of the concentration is the driving force for molecular transport in solution (Ruthven, 2008). Smittakorn et al. (2010) examined the influence of raising fluoride initial concentration on the removal efficiency a homemade bone char using synthetic water (1–6 mg/L) and field water samples (3.5 mg/L). Their findings revealed that both samples have almost the same removal capacity (0.130 and 0.157 mg/g, respectively) at 3.5 mg/L initial F⁻ concentration regardless to the availability of other ions in the field ground water, whilst F⁻ uptake declined after increasing the initial concentration to 6 mg/L (for the synthetic samples). In contrast, (Nasr et al., 2011) reported that increasing initial concentration from 2.5 to 10 mg/L resulted in a slight decrease in the adsorption capacity of cuttlefish bone char from 80% to 78% using a 15 g/L adsorbent dose and 1 h contact time. Increasing the bone char dose from 5 to 15 g/L enhanced the char uptake from 40 to 85%, but no more significant increases were noticed above 15 mg/L. Nevertheless, determining the removal capacity of the unit weight of the bone char shows that it removed fluoride of about 0.283 mg/g, which is less than the removal capacity of a thermally regenerated bone char (Kaseva, 2006). Similarly, Zhu et al. (2007) reported a removal capacity of 97% of F⁻ on Al doped cattle bone char at 1 mg/L F⁻ initial concentration and 10 g/L adsorbent dosage. The removal efficiency in this case is not representative of the adsorbent intake as it is equivalent to 0.97 mg/g F⁻ uptake, which is again less than the fluoride adsorption capacity of a commercial bone char (Leyva-Ramos et al., 2010; Medellin-Castillo et al., 2014; Medellin-Castillo et al., 2007). It is convenient to remark that adsorbent ability to uptake contaminants should be explained in unit weight of the substance adsorbed per unit weight of the adsorbent. This means, that the effect of initial concentration needs to be compared based on the adsorbent dose used in the experiments.

The percentage removal shows misleading results as it does not show the amount of adsorption sites occupied by the adsorbate. Different experimental conditions represented by the initial concentrations and bone char dose can significantly alter the results of F^- removal on bone char. For instance, Nasr et al. (2011) used 15 g/L bone char for the removal of 2.5–10 mg/L fluoride, which represents a high dose compared to the literature. Thus, the availability of more active sites on the adsorbent surface in solution eliminate the effect of the driving force due to the concentration gradient.

The effect of adsorbent dose was examined by Larsen et al. (1993) to remove 9.88 mg/L F^- from water using Ox bone char pyrolyzed at 580 °C. Increasing the bone char dose from 2.5 to 7.5 g/L resulted in decreasing fluoride concentrations in solution from 8.55 to about 5.5 mg/L. Sani et al. (2016) reported that fluoride removal efficiency increased significantly from 63.2 to 86.7% after increasing bone char dose from 4 to 10 g/L in batch experiments, but a contrary result where reported after calculating the uptake of fluoride per unit weight bone char 1.58 and 0.87 mg/g. This outcome is an indication for the reduction in the active sites available for occupying more F^- at higher solution concentrations.

3.3. Effect of pH value

Although most studies have examined fluoride removal from aqueous solution on bone char in neutral pH ranges (Leyva-Ramos et al., 2010; Nigri et al., 2017b; Zhu et al., 2007), the adsorption capacity of fluoride can be greatly influenced by change of pH range in the solution. The point of zero charge (pH_{PZC}), which represent the pH value at which the surface charge is zero, for bone char samples from different origins is reported to range between 7.4 and 10 (Ip et al., 2010; Medellin-Castillo et al., 2007; Nigri et al., 2017b). Medellin-Castillo et al. (2014) examined the effect of ionic strength on pH_{PZC} of a commercial bone char using 0.01 and 0.1 M NaCl. The results showed that increasing the ionic strength resulted in the raising the surface charge of the BC, but that the isoelectric point was not affected ($pH_{PZC} = 8.4$). In contrast, Dimović et al. (2009) reported that raising charring temperature will result in the raising of the surface charge and thus, the pH_{PZC} value from 7.37 to 10. Fluoride removal capacity will increase due to the interaction between the positively charged bone char surface (below pH_{PZC}) and negative fluoride ions. However, at very low pH values (< 3), bone char dissolution will occur and P will be released into the solution (Larsen et al., 1993) according to eq. (3) (Warren et al., 2009):

$$Ca_5(PO_4)_3OH + 7H^+ \rightarrow 5Ca^{2+} + 3H_2PO_4^- + H_2O \tag{3}$$

Bone char surface washing with acid solutions can enhance the removal capacity due to the protonation of the functional groups of the HAP at pH values lower than pH_{PZC} (as they mainly are > 7). Accordingly, protonation reactions will provide a positive charge to the surface and increase the affinity of F^- to the surface. Nigri et al. (2017b) reported that a maximum removal of 6.2 mg/g of F^- was achieved after washing a commercial bone char with 0.1 M HCl owing to the increase in the positive surface charge. Surface protonation followed the equations below (Medellin-Castillo et al., 2014):

$$\equiv P - OH + H^+ \rightarrow \equiv POH_2^+ \tag{4}$$

$$\equiv Ca - OH + H^+ \rightarrow \equiv Ca - OH_2^+ \tag{5}$$

Medellin-Castillo et al. (2007) investigated the impact of different pH values (3, 5, 7, 10, 11 and 12) on F^- removal from water using commercially produced granular cattle bone char (Fija Fluor) with a specific surface area of 104 m^2/g. The pH_{PZC} was reported to be about 8.4. Therefore, the maximum removal capacity (2.71 mg/g) at an initial F^- concentration of 1 mg/L was achieved at a low pH value (3.0). In addition, the authors found that the bone char removal capacity is 1.3 times smaller than a polymeric resin and greater than activated

aluminum and activated carbon by 2.8 and 36 times, respectively. Similarly, Abe et al. (2004) reported that there is a negative relationship between pH levels in solution and F^- removal capacity on bone char. A maximum F^- removal of 82% onto bone char surface was achieved with pH 4.6 (at 20 mg/L initial F^- concentration) when examining the effect of pH onto F^- removal capacity in the range between 4.6 and 9.2. It is noteworthy that, the surface charge of the adsorbent can significantly alter the removal capacity of fluoride on bone char. pH change affects the two adsorption mechanisms, i.e. electrostatic interaction and the chemical interaction resulting from the bone dissolution. Thus, shifting pH_{PZC} to acidic levels by altering the surface properties will provide a higher removal capacity of fluoride than at neutral pH levels.

3.4. Solution temperature

Different relationships between fluoride uptake on bone char and solution temperatures were reported in the literature. Abe et al. (2004) stated that fluoride uptake reaction on bone char is endothermic process due to the heat consumption during ion exchange process. Raising temperature from 9.85 to 39.85 °C had resulted in increasing the removal capacity of fluoride onto bone char from about 2.7 to 3.5 mg/g. Similar trend of reaction were reported by Zúñiga-Muro et al. (2017) examined the effect of temperature on fluoride uptake by Ce modified bone char. Increasing the temperature from 30 to 40 °C raised the removal capacity of the coated bone char by about 33% (13.6 mg/g), with an enthalpy change of 42 kJ/mol. The enthalpy change of fluoride adsorption reported by Rojas-Mayorga et al. (2015b) (26.67 kJ/mol) also indicated an endothermic reaction of fluoride adsorption onto Al(III) doped bone char. By contrast, a much lower enthalpy change (< 8.36 kJ/mol) was reported by Medellin-Castillo et al. (2007), which indicated that increasing temperature from 15 to 35 °C had no effect on fluoride uptake using commercial bone char. These different results are due to the difference in the ion exchange performance of fluoride with available ions on bone char or coated bone char (coating with metal). It is also noteworthy to remark that the increase in the solution temperature will increase the solubility of the metal oxides coated on bone char surface and thus, alter the removal capacity of F^- from solution. In addition, based on the ionic strength of the solution, the changes in the zeta potential of adsorbent due to changing solution temperature may affect the performance of the adsorbent to remove contaminants from solution.

On the other hand, an exothermic behavior of the fluoride adsorption on aluminum sulfate and calcium oxide treated bone char, with a negative enthalpy change of -44.8 kJ/mol, was observed by Chatterjee et al. (2018). Increasing solution temperature from 30 °C to 50 °C resulted in a decrease in fluoride uptake from 25 to 10 mg/g, which was related to the inverse relationship between mass transfer coefficient and temperature (9×10^{-4} and 8.5×10^{-4} m/s at 30 and 50 °C, respectively). The effective diffusivity of fluoride ions in solution within the pores was reported to be unaffected by the change of the solution temperature (5.8×10^{-12} and 6.2×10^{-12} m^2/s at 30 and 50 °C, respectively). The effect of solution temperature on fluoride adsorption lies in its effect on the balance of the adsorbent-adsorbate system, which in turn shifts the position of the equilibrium to counter this change.

3.5. Adsorbent particle size

Adsorbent particle size is an important factor that affects the adsorption capacity and rate of fluoride adsorption from aqueous solution. Particle size also plays an important role in altering the rate and capacity of fluoride adsorption. Chatterjee et al. (2018) demonstrated that when the size of carbonized bone meal particles decreased from 0.5 mm to 0.15 mm, the fluoride adsorption capacity showed an increase from 12 to 14 mg/g. Similarly, Kaseva (2006) also reported that a decrease of

bone char particle size produced from cattle bones resulted in an increase in fluoride adsorption from water. The examinations were made using different ranges of particle sizes. The residual fluoride decreased from 15.2 mg/L to 11.26 mg/L after a contact time of 120 min using 2.5–3 and 0.5–1.0 mm particle size, respectively. Similar results have also been reported by Zhu et al. (2011) who observed that the smaller the grain particle, the higher the removal efficiency of the bone char filter, and recorded a maximum of 70.64% F^- removal from drinking water. Thus, reducing the bone char particle size increases the effective surface area, provides more active sites for fluoride removal and eases the diffusivity of the adsorbate to penetrate the pores of the adsorbent (Gupta et al., 2011). However, for water treatment applications (filters) it is quite important to have a suitable particle size distribution in order to avoid clogging issues. On the other hand, large particles may provide a suitable environment for bacterial growth on carbon particles due to the availability of high surface area, pores and functional groups (Lin et al., 2010). The study reported an increase in the particle size in the effluent from 5 to 25 μm after filtration. The accumulation of organics and bacteria on the porous surface of activated carbon provided a good environment for microorganism growth. Consequently, biodegradation of the organics attached to the surface and of the functional groups of the carbon surface occurred and the newly attached particles to the carbon surface were separated from the carbon surface to form larger particles in the effluent. The latter desired more strength against chlorine disinfection due to the presence of extensive bacterial colonization in the large porous particles. Furthermore, there was an increase in anion concentrations (due to bacterial effect) and metallic substance in the effluent. Thus, optimizing the size range of particles is a necessity for fluoride removal via filtration, as it could act as a suitable environment for microorganism growth.

4. Adsorption isotherms

Aquatic system equilibrium is based on the law of thermodynamics, which provides an estimation of particles transport and reactivity in the system. Estimations of the final composition of a system after all reactions have occurred is based on thermodynamic approaches (Mason, 2013). Thus, the ability of different adsorbents to uptake contaminants varies based upon adsorption isotherm models (Smittakorn et al., 2010). The latter are usually determined by equilibrating the solution with varying concentrations of solid particles (contaminants). According to Barakat (2011), the sorption process follows three stages; mainly (i) the transport of contaminants from the liquid to solid surface, (ii) adsorption on the sorbent media particles, and (iii) finally the substance transport within the sorbent particles. Howe et al. (2012) described adsorption as an equilibrium reaction in which the adsorbate distributes between the adsorbent and the solution according to an adsorption isotherm. An adsorption isotherm is a curve constructed from measurements of progressive adsorption at reaction equilibrium at constant pH and temperature. As illustrated in Table 4, different isotherm models were used to predict the adsorption of contaminants from water/wastewater onto sorbents.

Langmuir and Freundlich isotherm models have commonly been applied to describe the equilibrium adsorption of fluoride by bone char. The Langmuir model assumes that all adsorption sites are identical and therefore, there is an equivalent affinity between each adsorbate and adsorbent molecules. Accordingly, the reaction enthalpy and sorption activation energy are constant. This model can be applied to monolayer adsorption with even distribution of heat and affinities when adsorption occurs over the homogeneous surface (Langmuir, 1918). On the other hand, the Freundlich isotherm model assumes a non-ideal, reversible multilayer adsorption process on a heterogeneous adsorbent surface (Foo and Hameed, 2010). Generally, the simulation of the isotherm model of fluoride on bone char in recent studies was based on Langmuir and Freundlich models. However, in rare cases, some other models were examined such as Sips, Dubinin-Radushkevich and Radke-

Prausnitz isotherms. Sani et al. (2016) reported that adsorption of F^- onto bone char followed the Langmuir model, which indicated that the adsorption mechanism followed monolayer adsorption. Medellin-Castillo et al. (2007) applied the Langmuir and Freundlich isotherms to describe the adsorption equilibrium data of F^- on bone char. The results showed that the adsorption behavior of F^- removal on a commercial bone char was well presented by both models. However, the results of Freundlich model were more representative at high F^- concentrations. Similarly, Abe et al. (2004) found that the experimental data of F^- was fitted well to use of the Freundlich isotherm.

The Sips model is a combination of the Langmuir and Freundlich isotherm models and can better describe the adsorption process on heterogeneous surfaces (Günay et al., 2007). Fluoride removal on Ce^{4+} modified bone char was best fitted to the Sips model indicating the availability of more than one binding sites (Ca^{2+} and Ce^{4+}) on the surface (Zúñiga-Muro et al., 2017). For a commercial bone char, Tovar-Gómez et al. (2013) reported that both the Langmuir and Sips isotherms were best determined the isotherm of F^- removal compared to the Freundlich model.

Based on the adsorbate concentration, Radke-Prausnitz isotherm model can be reduced to linear model change to the Freundlich or Langmuir model (Ayawei et al., 2017). It best fits the data at low adsorbate concentration. With regards to F^- removal on commercial bone char, Radke-Prausnitz best fitted the data since it is a three parameters model compared to the Langmuir and Freundlich isotherm models (Leyva-Ramos et al., 2010). Medellin-Castillo et al. (2014) used Langmuir, Freundlich and Radke-Praustniz models to investigate the adsorption equilibrium of F onto commercial bone chat. The results implied that the Radke-Praustniz model well fitted the adsorption data based on the lower average absolute percentage deviation obtained values from the Radke-Praustniz compared to those obtained by the other two models.

Chatterjee et al. (2018) applied three isotherms (including Langmuir, Freundlich and Dubinin–Radoshkevitch models) to describe the adsorption equilibrium data of F^- on chemically treated carbonized bone meal followed the Langmuir model, and found that the experimental data was fitted better at different temperatures by the Langmuir model than by other models.

Nigri et al. (2017a) found that the adsorption of F^- with thermally regenerated bovine bone char followed the Freundlich and Redlich-Peterson isothermal plots well when compared to the results achieved by applying Langmuir, Temkin and Sips isotherms. The higher R^2 of 0.9964 of the Freundlich isotherm suggested that the adsorption took place on the heterogeneous surface of the adsorbent.

The mechanism for F^- ion removal onto HAP, which is the effective component of the bone char, was attributed to either surface sorption, substitution or precipitation depending on the reaction conditions (Sternitzke et al., 2012). However, the mechanism is dependent on the F^- initial concentration in solution (Sani et al., 2016). The general consensus suggests that fluoride removal on bone char mostly followed an ion exchange process between F^- and hydroxyl ions to compose fluorapatite (Abe et al., 2004; Kawasaki et al., 2009; Medellin-Castillo et al., 2014). Hence the isotherm that best correlates with these reactions would be the best fit for describing fluoride removal using bone char. The suitability of a model to represent the isotherm of F^- removal from water may also be related to the availability of the active sites on the surface of the adsorbent particles, in which the diffusion of the F^- will occur after the surface sites become less available (which is again related to the adsorbent-adsorbate ratio of the system).

5. Effect of oxyanions on fluoride removal

Medellin-Castillo et al. (2007) examined the impeding effect of chloride, nitrate, nitrite, sulfate and phosphate in natural water on fluoride removal. Examining the concentration of the anions in solution after the adsorption process showed that there was no decrease in the

Table 4
List of some isotherm models (Foo and Hameed, 2010).

Isotherm	Nonlinear form	Linear Form	Plot
Langmuir	$q_e = \frac{Q_0 b C_e}{1 + b C_e}$	$\frac{C_e}{q_e} = \frac{1}{bQ_0} + \frac{C_e}{Q_0}$	$\frac{C_e}{q_e}$ vs C_e
		$\frac{1}{q_e} = \frac{1}{Q_0} + \frac{1}{bQ_0 C_e}$	$\frac{1}{q_e}$ vs $\frac{1}{C_e}$
		$q_e = Q_0 - \frac{q_e}{bC_0}$	q_e vs $\frac{q_e}{bC_0}$
		$\frac{q_e}{C_e} = bQ_0 - bq_e$	$\frac{q_e}{C_e}$ vs q_e
Freundlich	$q_e = K_F C_e^{1/n}$	$\log q_e = \log K_F + \frac{1}{n}\log C_e$	$\log q_e$ vs $\log C_e$
Dubinin–Radushkevich	$q_e = (q_s)\exp(-k_{ad}\varepsilon^2)$	$\ln(q_e) = \ln(q_s) - k_{ad}\varepsilon^2$	$\ln(q_e)$ vs ε^2
Tempkin	$q_e = \frac{RT}{b_T}\ln A_T C_e$	$q_e = \frac{RT}{b_T}\ln A_T + \left(\frac{RT}{b_T}\right)\ln C_e$	q_e vs C_e
Flory-Huggins	$\frac{\theta}{C_0} = K_{FH}(1-\theta)^{n_{FH}}$	$\log\left(\frac{\theta}{C_0}\right) = \log(K_{FH}) + n_{FH}\log(1-\theta)$	$\log\left(\frac{\theta}{C_0}\right)$ vs $\log(1-\theta)$
Hill	$q_e = \frac{q_{sH} C_e^{n_H}}{K_D + C_e^{n_H}}$	$\log\left(\frac{q_e}{q_{sH} - q_e}\right) = n_H\log(C_e) - \log(K_D)$	$\log\left(\frac{q_e}{q_{sH} - q_e}\right)$ vs $\log(C_e)$
Redlich-Peterson	$q_e = \frac{K_R C_e}{1 + a_R C_e^g}$	$\ln\left(K_R\frac{C_e}{q_e} - 1\right) = g\ln(C_e) + \ln(a_R)$	$\ln\left(K_R\frac{C_e}{q_e} - 1\right)$ vs $\ln(C_e)$
Sips	$q_e = \frac{K_S C_e^{\beta s}}{1 + a_S C_e^{\beta s}}$	$\beta\ln(C_e) = -\ln\left(\frac{K_S}{q_e}\right) + \ln(a_S)$	$\ln\left(\frac{K_S}{q_e}\right)$ vs $\ln(C_e)$
Toth	$q_e = \frac{K_T C_e}{(a_T + C_e)^{1/t}}$	$\ln\left(\frac{q_e}{K_T}\right) = \ln(C_e) - \frac{1}{t}\ln(a_T + C_e)$	$\ln\left(\frac{q_e}{K_T}\right)$ vs $\ln(C_e)$
Koble–Corrigan	$q_e = \frac{A C_e^n}{1 + B C_e^n}$	$\frac{1}{q_e} = \frac{1}{A C_e^n} + \frac{B}{A}$	–
Khan	$q_e = \frac{q_s b_K C_e}{(1 + b_K C_e)^{a_K}}$	–	–
Radke–Prausnitz	$q_e = \frac{a_{RP} r_R C_e^{\beta_R}}{a_{RP} + r_R C_e^{\beta_R - 1}}$	–	–
BET	$q_e = \frac{q_S C_{BET} C_e}{(C_S - C_e)[1 + (C_{BET} - 1)(C_e / C_S)]}$	$\frac{C_e}{q_e(C_S - C_e)} = \frac{1}{q_S C_{BET}} + \frac{(C_{BET} - 1)}{q_S C_{BET}}\frac{C_e}{C_S}$	$\frac{C_e}{q_e(C_S - C_e)}$ vs $\frac{C_e}{C_S}$
FHH	$\ln\left(\frac{C_e}{C_S}\right) = -\frac{\alpha}{RT}\left(\frac{q_s}{q_e d}\right)^r$	–	–
MET	$q_e = q_s\left(\frac{k}{\ln(C_S / C_e)}\right)^{1/3}$	–	–

concentration, indicating that the presence of these anions had no effect on F^- uptake on bone char. On the other hand, adsorption experiments showed a reduction in the carbonate concentration indicating a competition with F^- ions on the bone char surface. However, the higher amount of F^- adsorbed compared to the carbonate, confirmed that the bone char surface would selectively remove F^- rather than carbonate. The same results were confirmed by Medellin-Castillo et al. (2014) while investigating the influence of these anions. The decrease of anion affinities toward bone char (at concentration < 0.3 meq/L) was in the following order $F^- > Cl^- > CO_3^{2-} > NO_2^- \approx NO_3^- \approx HCO_3^- \approx SO_4^{2-}$. Smittakorn et al. (2010) also reported that the presence of anions had no effect on F^- removal on Thai bone char, but the presence of cations such as aluminum and magnesium will contribute by enhancing the defluoridation process from water due to the formation of complexes that easily precipitate on the char surface. Similarly, Abe et al. (2004) reported that the presence of NaCl salts in water improved the uptake of F^- from water due to the hydration of dissolute NaCl salts, providing a lower potential of F^- dissolution in water. Increasing the ionic strength from 0.01 to 1 M resulted in increasing the removal capacity of F^- on bone char from about 2.75 to 3.86 mg/g. The increase in the adsorption of F^- with increasing ionic strength could be attributed to the effect of the latter on reducing the electric double layer leading to better electrostatic interaction (Al-Juboori et al., 2016a). Larsen et al. (1993) compared the effectiveness of ox bone char to remove F^- from water with and without the presence of brushite (BSH) and calcium hydroxide, reporting that the removal capacity of the bone char increased from 0.64 to 3.88 mg/g after adding 0.05 g BSH and 0.015 g Ca(OH)$_2$ to the solution.

The simultaneous removal of As and F^- using bone char was also investigated in a recent research, reporting the suitability of fish bone charred at 500 °C for the simultaneous removal of As(V) and F^- from water. However, a higher removal capacity of fluoride was achieved due to exchanging ions between hydroxyapatite composition of the bone char and fluoride ions in solution.

6. Regeneration

Regeneration capacity is of utmost importance to evaluate the reusability of bone char efficiency in the removal of contaminants from water. Regeneration of bone char could provide recovery of pollutants, reusability of adsorbents, reducing the process cost and reducing wastes to be processed. Kaseva (2006) examined the effect of thermal regeneration in the temperature range of 100–800 °C, with regeneration time of (30–240 min) on the bone char efficiency for fluoride removal from water. Kaseva (2006) proposed the release of hydrogen fluoride (HF) gas from saturated bone char upon exposure to thermal treatment as a regeneration mechanism. Technically, this can probably happen when there is a source of hydrogen to react with fluoride.

The result showed that the F^- adsorption capacity of the regenerated bone char increased from 0.2 to 0.75 mg/g after raising the regeneration temperature from 100 to 500 °C for 120 min residence time. However, further increases in the regeneration temperature resulted in decreasing the uptake capacity of F^- on bone char. Nigri et al. (2017a) examined the effect of thermal regeneration on bovine commercial bone char at different temperatures. The results of X-ray diffraction (XRD) showed the presence of F^- ions in the structure of the bone char after regeneration, but the composition of the bone char was not altered by applying thermal treatment. This contradicts with the proposed regeneration mechanism of Kaseva (2006) where fluoride is suggested to be released in a form of HF gas. Fluoride diffusion seems to be more acceptable in explaining the thermal regeneration of bone char as opposed to HF formation especially if there is no source of hydrogen whether directly applied or released due to chemical reactions. The optimum conditions for the regeneration in the study by Nigri et al.

(2017a) were different from the results reported by Kaseva (2006) as the experimental conditions were different. The optimum temperature for the regeneration process of the bone char was 400 °C resulting in 2.25 mg/g F⁻ uptake capacity.

Chatterjee et al. (2018) reported that F⁻ uptake on chemically treated carbonized bone meal was decreased by 18% and 31% in the second and third cycle respectively, after regenerating the adsorbent with 0.1 M NaOH. Medellin-Castillo et al. (2007) examined the desorption of fluoride from commercial bone char by placing the adsorbent in water at pH values of 7 and 12. Fluoride desorption at pH 12 performed better than neutral pH due to the abundant availability of exchangeable hydroxyl groups, indicating a reversible F⁻ adsorption process. On a large scale, the most efficient regeneration process for bone char was reported by the use of 1–2 M NaOH solution for the regeneration of 2500 L of saturated bone char (Catholic Diocese of Nakuru, Water Quality, and Muller, 2007). The intermittent flushing of the bone char with NaOH is followed by washing with water to reduce the pH of the outflow and then suppling CO_2 enriched water to lower the pH below 8. The waste water generated from the regeneration process were precipitated with CaOH or $CaCl_2$ to form CaF_2, which have low solubility and can retain fluoride. The cost of the process was reported to be around $ 280 USD (339.27 USD in 2019 after adding the inflation rate)

The disposal of the concentrated fluoride solution resulting from the bone char regeneration can be a challenge. Such a problem can be overcome by recycling the concentrated fluoride into green industries. Zhu et al. (2013) used calcium fluoride sludge for producing strong corrosion resistant ceramic that locks fluoride well and prevents it from leaching out of the structure. In another study, fluorapatite was applied as a reusable catalyst in solvent-free epoxidation (Ichihara et al., 2003).

7. Bone char defluoridation units -existing and conceptual designs

After discussing the factors affecting bone char defluoridation efficiency, it is important to look into the designs of units used in such applications. Most of the designs available were developed to be affordable and practical for low economic and remote communities. Examples of the most common designs used for defluoridation are illustrated in Fig. 5. Fawell et al. (2006) compared the advantages and disadvantages of these designs and the column was found to be the best one. Some more sophisticated designs were also implemented in Africa and India where bone char was used in a bed configuration for the precipitation of fluoride with calcium (Nalgonda technique), this technique is termed as contact precipitation (Ayoob et al., 2008). Theses designs were commercialized and are readily available for communities at affordable prices (Kinyua, 2016). An example for the commercial supplier for these designs is the Nakuru Deflouridation Company in Kenya using bone from many different sources such as goat, camel, cattle and sheep bones (Nakuru Defluoridation Company Ltd). The challenge with these simple designs is monitoring fluoride removal levels and the adsorption capacity of the char throughout the operation period. In 2005, the Catholic Diocese of Nakuru, Water Quality (CDN WQ) (Catholic Diocese of Nakuru, Water Quality, and Muller, 2007) adopted a new design of a kiln to produce about 10 tons bone char per batch using animal bones from different sources. The best defluoridation process was reported to be with bone char produced at 400 °C for 1–5 days. To improve the quality of the produced bone char, the outlet of the air and the amount of the oxygen entering the kiln was controlled by adjusting the size of the chimney and reusing the air of the outlet by mixing it with a limited amount of oxygen. The regeneration processes of bone char used in these designs has to be done with relatively strong alkaline solution which would be problematic to handle and store especially when the setups used in village communities. This means that researching more advanced designs is inevitable.

In this study, we propose some conceptual designs that have the capacity to prolong bone char adsorption capacity and are self-cleaning as shown in Fig. 6. As it can be seen from this figure, column configuration is used in both designs. The designs apply electrical and ultrasonic enhancing adsorption mechanisms. The electric-enhancing column should be made of non-conductive material (e.g. plastic), while the ultrasonic-enhancing column should be made of magnetostrictive materials (e.g. nickel) due to its efficiency in generating ultrasonic vibration (Al-Juboori et al., 2016b). It is noteworthy that the two designs require only low level of electrical power which can be sourced from solar energy. For example, applying electrolysis should not exceed the low voltage of 1.23 V as water electrolysis occurs beyond this level (Qi,
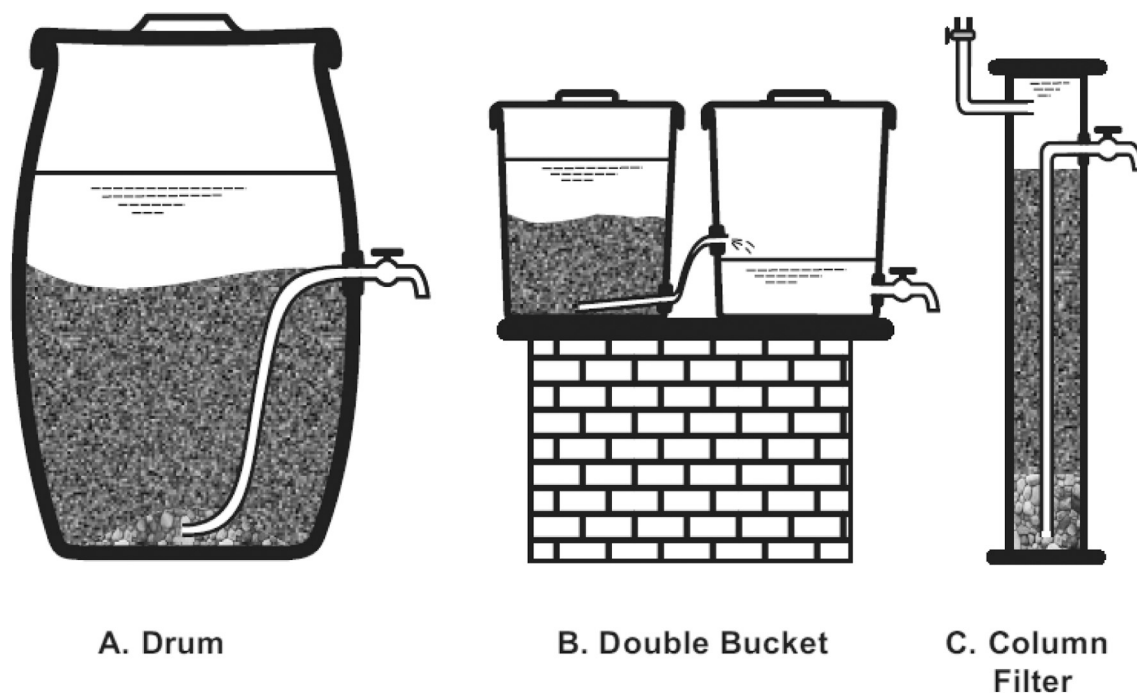

A. Drum **B. Double Bucket** **C. Column Filter**

Fig. 5. Most common domestic units designs for defluoridation in developing countries (Fawell et al., 2006).
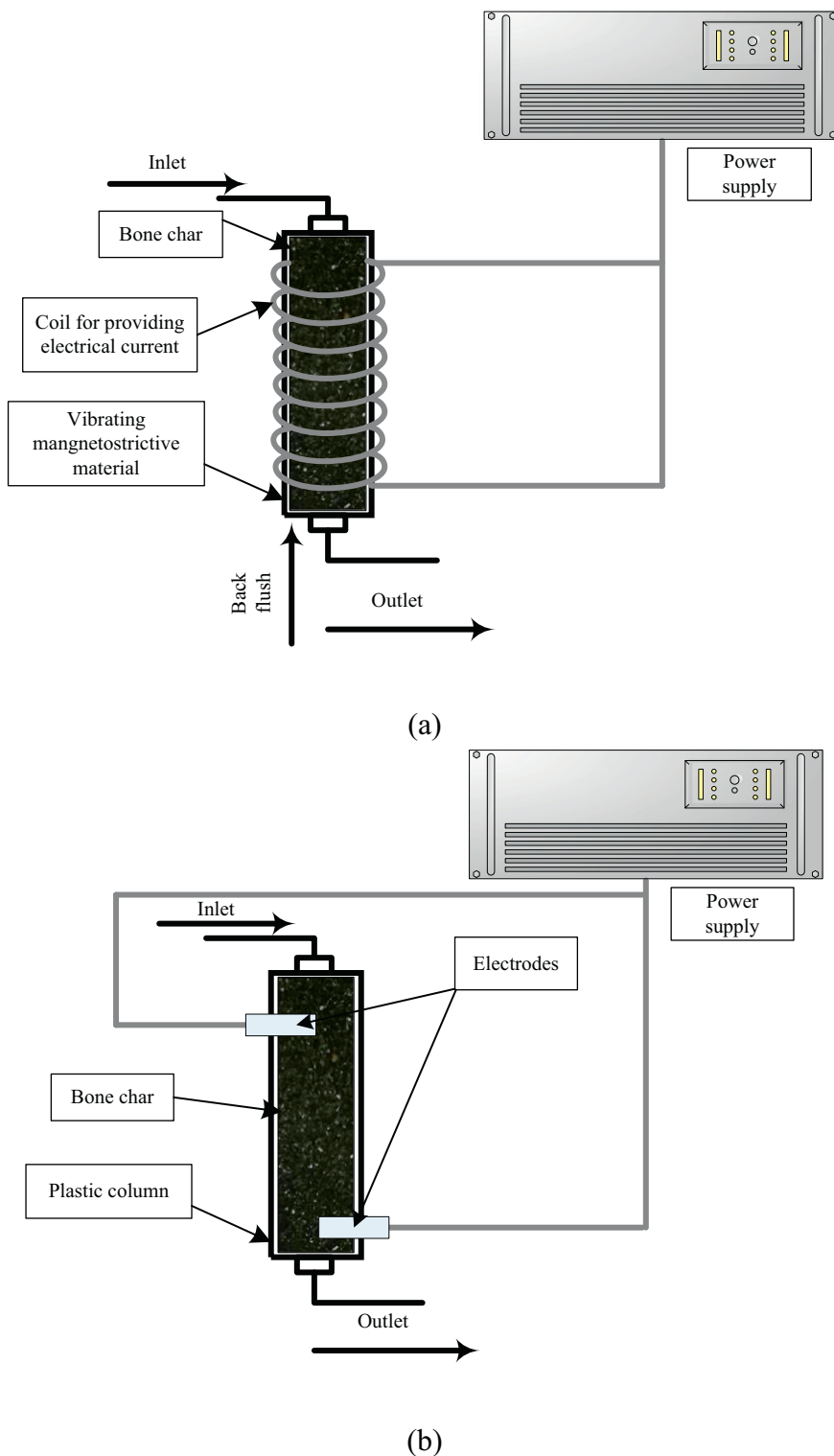
Fig. 6. Conceptual designs for bone char columns: a) ultrasonically enhanced adsorption and b) electrically enhanced adsorption.

2013). Similarly, only low level of energy is required for vibrating magnetostrictive materials with ultrasound. For instance, the domain wall energy for iron is $1.1 \times 10^{-3} \, J/m^2$ (Thoelke, 1993). It is hard to indicate energy demands for the proposed designs as these figures depend on several factors such as size of the column, quality of the char, flowrate, thickness of the column, number of the coil turns, etc. The electrically enhanced adsorption design promotes the electrostatic mechanisms of fluoride adsorption onto the char by the small voltage applied through the electrodes. To make the design more environmentally friendly, these electrodes can be used from recycled batteries and this in turn would reduce batteries disposal problem. The electrically enhanced adsorption design can be regenerated by charge reversal. The ultrasonically enhanced adsorption design relies on reducing the dead area of the char particles resulting from packing and prevents the formation of channels in column bed due to the continuous vibration. This design can be regenerated by back flush with treated

water applying the same or slightly higher vibration level as that used with adsorption.

8. Conclusion and future directions

The health concerns associated with the high fluoride concentration in drinking water sources were highlighted in this study. Due to the feasibility of bone char as a green adsorbent for fluoride removal, a comprehensive review addressing all the important aspects of this technology was provided. The optimum temperature range and production conditions for bone char were evaluated. Bone char samples produced at 500–700 °C seem to have the best defluoridation capacity. In addition, the effectiveness of coating with multivalent ions and the experimental conditions for batch and column filtrations were discussed. Among all coating cations, aluminum appears to be promising for increasing the removal capacity of F^- removal from water. Despite these findings, further studies are required to optimize the rate of fluoride removal on bone char as most of the studies showed that equilibrium was achieved after 24 h. The possibility of regenerating bone char and the reduction of solid waste justify the energy requirements for bone char production processes. In the case of gasification, energy for bone char production can be compensated by syngas generation. The recent low commercial price of bulk bone char indicates the drop in the cost production of the char. Possible utilization of concentrated fluoride generated from bone char regeneration for green industry application was also suggested. Challenges with existing domestic defluoridation designs were pinpointed and new conceptual designs were discussed.

More extensive works are required to examine the effective particle size for fluoride removal using column filters to avoid issues related to bacterial growth through filter layers. Further investigations are also required to examine the removal of fluoride from industrial wastewater as it can form more complex compounds due to the presence of high fluoride concentrations of various contaminants in the wastewater system. Research into the proposed defluoridation designs would be beneficial for the advancement of removal technologies.

Acknowledgements

References

Abaei, Z., Faghihian, H., Esmaeeli, N., 2017. Preparation and application of zeolitic adsorbents for removal of fuoride from aqueous solution; equilibrium, kinetic and thermodynamic studies. Der Chemica Sinica 8 (6), 524–534.

Abe, I., Iwasaki, S., Tokimoto, T., Kawasaki, N., Nakamura, T., Tanada, S., 2004. Adsorption of fluoride ions onto carbonaceous materials. J. Colloid Interface Sci. 275 (1), 35–39.

Alibaba.com Sky Bone Ash PVT from Russian Federation Inc. https://m.alibaba.com/amp/product/133373450.html.

Al-Juboori, R.A., Yusaf, T., Aravinthan, V., Pittaway, P.A., Bowtell, L., 2016a. Investigating the feasibility and the optimal location of pulsed ultrasound in surface water treatment schemes. Desalin. Water Treat. 57 (11), 4769–4787.

Al-Juboori, R.A., Bowtell, L.A., Yusaf, T., Aravinthan, V., 2016b. Insights into the scalability of magnetostrictive ultrasound technology for water treatment applications. Ultrason. Sonochem. 28, 357–366.

Arrenberg, A., 2010. Production Models for Bone Char Defluoridation. Naivsha, Kenya. MSc Thesis. Cranfield University School of Applied Sciences, Cranfield, UK.

Ayawei, N., Ebelegi, A.N. and Wankasi, D. (2017) Modelling and interpretation of adsorption isotherms. J. Chem. (Hindawi) 2017, ID 3039817.

Ayoob, S., Gupta, A., Bhat, V.T., 2008. A conceptual overview on sustainable technologies for the defluoridation of drinking water. Crit. Rev. Env. Sci. Tec. 38 (6), 401–470.

Barakat, M., 2011. New trends in removing heavy metals from industrial wastewater. Arab. J. Chem. 4 (4), 361–377.

Brunson, L.R., Sabatini, D.A., 2009. An evaluation of fish bone char as an appropriate arsenic and fluoride removal technology for emerging regions. Environ. Eng. Sci. 26 (12), 1777–1784.

Bulk Bone Char® Promolife Inc. https://www.promolife.com/bulk-bone-char-for-water-filter-systems/.

Cai, Q., Turner, B.D., Sheng, D., Sloan, S., 2017. Application of kinetic models to the design of a calcite permeable reactive barrier (PRB) for fluoride remediation. Water Res. 130, 300–311.

Catholic Diocese of Nakuru, Water Quality, Muller, K., 2007. CDN's Experiences in Producing Bone Char. Catholic Diocese of Nakuru, Nakuru, Kenya and Swiss Federal Institute of Aquatic Science and Technology (EAWAG), Dübendorf, Switzerland.

Çeçen, F., Aktas, Ö., 2011. Activated Carbon for Water and Wastewater Treatment: Integration of Adsorption and Biological Treatment. John Wiley & Sons.

Changmai, M., Pasawan, M., Purkait, M., 2018. A hybrid method for the removal of fluoride from drinking water: parametric study and cost estimation. Sep. Purif. Technol. 206, 140–148.

Chatterjee, S., Mukherjee, M., De, S., 2018. Defluoridation using novel chemically treated carbonized bone meal: batch and dynamic performance with scale-up studies. Environ. Sci. Pollut. R 25, 18161–18178.

Cheung, C., Chan, C.K., Porter, J.F., McKay, G., 2001a. Film-pore diffusion control for the batch sorption of cadmium ions from effluent onto bone char. J. Colloid Interf. Sci. 234 (2), 328–336.

Cheung, C., Porter, J., McKay, G., 2001b. Sorption kinetic analysis for the removal of cadmium ions from effluents using bone char. Water Res. 35 (3), 605–612.

Chigondo, M., Paumo, H.K., Bhaumik, M., Pillay, K., Maity, A., 2018. Rapid high adsorption performance of hydrous cerium-magnesium oxides for removal of fluoride from water. J. Mol. Liq. 265, 496–509.

Dahi, E., 2016. Africa's U-turn in defluoridation policy: from the Nalgonda technique to bone char. Fluoride 49 (4), 401–416.

Delgadillo-Velasco, L., Hernández-Montoya, V., Cervantes, F.J., Montes-Morán, M.A., Lira-Berlanga, D., 2017. Bone char with antibacterial properties for fluoride removal: preparation, characterization and water treatment. J. Environ. Manag. 201, 277–285.

Dewage, N.B., Liyanage, A.S., Pittman Jr., C.U., Mohan, D., Mlsna, T., 2018. Fast nitrate and fluoride adsorption and magnetic separation from water on α-Fe₂O₃ and Fe₃O₄ dispersed on Douglas fir biochar. Bioresour. Technol. 263, 258–265.

Dimović, S., Smičiklas, I., Plećáš, I., Antonović, D., Mitrić, M., 2009. Comparative study of differently treated animal bones for Co²⁺ removal. J. Hazard. Mater. 164 (1), 279–287.

Edmunds, W.M., Smedley, PL., 2013. Fluoride in natural waters. Ch 13. Revised edition In: Selinus, O, Alloway, B, Centeno, J A, Finkelman, RB, Fuge, R, Lindh, U, Smedley, PL. (Eds.), Essentials of Medical Geology. Springer, pp. 311–336.

Elango, L., Jagadeshan, G., 2018. Clean and Sustainable Groundwater in India. Springer, pp. 13–23.

Fawell, J.K., Bailey, K., Chilton, J., 2006. Fluoride in drinking-water. World Health Organization, Geneva, Switzerland.

Field, R.A., Riley, M., Mello, F., Corbridge, J., Kotula, A., 1974. Bone composition in cattle, pigs, sheep and poultry. J. Anim. Sci. 39 (3), 493–499.

Figueiredo, M., Fernando, A., Martins, G., Freitas, J., Judas, F., Figueiredo, H., 2010. Effect of the calcination temperature on the composition and microstructure of hydroxyapatite derived from human and animal bone. Ceram. Int. 36 (8), 2383–2393.

Foo, K.Y., Hameed, B.H., 2010. Insights into the modeling of adsorption isotherm systems. Chem. Eng. J. 156 (1), 2–10.

Goodman, P.A., Li, H., Gao, Y., Lu, Y., Stenger-Smith, J., Redepenning, J., 2013. Preparation and characterization of high surface area, high porosity carbon monoliths from pyrolyzed bovine bone and their performance as supercapacitor electrodes. Carbon 55, 291–298.

Günay, A., Arslankaya, E., Tosun, I., 2007. Lead removal from aqueous solution by natural and pretreated clinoptilolite: adsorption equilibrium and kinetics. J. Hazard. Mater. 146 (1–2), 362–371.

Gupta, V., Gupta, B., Rastogi, A., Agarwal, S., Nayak, A., 2011. A comparative investigation on adsorption performances of mesoporous activated carbon prepared from waste rubber tire and activated carbon for a hazardous azo dye—Acid Blue 113. J. Hazard. Mater. 186 (1), 891–901.

Hansen, S.P., Gumerman, R.C., Culp, R.L., 1979. Estimating Water Treatment Costs: Cost Curves Applicable to 2,500 gpd to 1 mgd Treatment Plants. US Environmental Protection Agency.

Harrison, P.T., 2005. Fluoride in water: a UK perspective. J. Fluor. Chem. 126 (11−12), 1448–1456.

Herath, H., Kawakami, T., Tafu, M., 2018. Repeated heat regeneration of bone char for sustainable use in fluoride removal from drinking water. Healthcare (Basel) 6 (4), 143.

Howe, K.J., Crittenden, J.C., Hand, D.W., Trussell, R.R., Tchobanoglous, G., 2012. Principles of Water Treatment, 3ʳᵈ edition. John Wiley & Sons.

Ichihara, J., Kambara, A., Iteya, K., Sugimoto, E., Shinkawa, T., Takaoka, A., Yamaguchi, S., Sasaki, Y., 2003. Cetylpyridinium dodecatungstate on fluorapatite: efficient and reusable solid catalyst for solvent-free epoxidation. Green Chem. 5 (5), 491–493.

Ip, A.W., Barford, J.P., McKay, G., 2010. A comparative study on the kinetics and mechanisms of removal of Reactive Black 5 by adsorption onto activated carbons and bone char. Chem. Eng. J. 157 (2–3), 434–442.

Ishikawa, K., Miyamoto, Y., Tsuchiya, A., Hayashi, K., Tsuru, K., Ohe, G., 2018. Physical and histological comparison of hydroxyapatite, carbonate apatite, and β-tricalcium phosphate bone substitutes. Materials (Basel) 11 (10) (12 pages).

Ismail, Z.Z., AbdelKareem, H.N., 2015. Sustainable approach for recycling waste lamb and chicken bones for fluoride removal from water followed by reusing fluoride-bearing waste in concrete. Waste Manag. 45, 66–75.

Jackson, P., Harvey, P., Young, W., 2002. Chemistry and Bioavailability Aspects of Fluoride in Drinking Water. WRc-NSF, Marlow, Buckinghamshire.

Jeihanipour, A., Shen, J., Abbt-Braun, G., Huber, S.A., Mkongo, G., Schäfer, A.I., 2018. Seasonal variation of organic matter characteristics and fluoride concentration in the Maji ya Chai River (Tanzania): impact on treatability by nanofiltration/reverse osmosis. Sci. Total Environ. 637, 1209–1220.

Kader, A.A., Aly, A., Girgis, B., 1996. Bone char decolorisation efficiency. A laboratory study over four consecutive cycles. Int. Sugar J. (Worldwide Sugar Edition) 98 (1174), 542–554.

Karmakar, S., Bhattacharjee, S., De, S., 2017. Experimental and modeling of fluoride removal using aluminum fumarate (AlFu) metal organic framework incorporated cellulose acetate phthalate mixed matrix membrane. JECE 5 (6), 6087–6097.

Kaseva, M., 2006. Optimization of regenerated bone char for fluoride removal in drinking water: a case study in Tanzania. J. Water Health 4 (1), 139–147.

Kawasaki, N., Ogata, F., Tominaga, H., Yamaguchi, I., 2009. Removal of fluoride ion by bone char produced from animal biomass. J Oleo Sci 58 (10), 529–535.

Keene, B., Knowlton, K., McGilliard, M., Lawrence, L., Nickols-Richardson, S., Wilson, J., Rutledge, A., McDowell, L., Van Amburgh, M., 2004. Measures of bone mineral content in mature dairy cows. J. Dairy Sci. 87 (11), 3816–3825.

Kinyua, L., 2016. A Study of Defluoridation Techniques and the Current State of Defluoridation in Kenya. BSc Thesis. University of Nairobi, Nairobi, Kenya.

Lai, Y.-q., Kai, Y., Chao, Y., Tian, Z.-l., Guo, W.-c., Jie, L., 2018. Thermodynamics and kinetics of fluoride removal from simulated zinc sulfate solution by La (III)-modified zeolite. T. Nonferr. Metal Soc. 28 (4), 783–793.

Lambert, S., Graham, N., 1989. Adsorption methods for treating organically coloured upland waters. Environ. Technol. 10 (9), 785–798.

Langmuir, I., 1918. The adsorption of gases on plane surfaces of glass, mica and platinum. J. Am. Chem. Soc. 40 (9), 1361–1403.

Larsen, M., Pearce, E., Jensen, S., 1993. Defluoridation of water at high pH with use of brushite, calcium hydroxide, and bone char. J. Dent. Res. 72 (11), 1519–1525.

Leyva-Ramos, R., Rivera-Utrilla, J., Medellin-Castillo, N., Sanchez-Polo, M., 2010. Kinetic modeling of fluoride adsorption from aqueous solution onto bone char. Chem. Eng. J. 158 (3), 458–467.

Lhassani, A., Rumeau, M., Benjelloun, D., Pontie, M., 2001. Selective demineralization of water by nanofiltration application to the defluorination of brackish water. Water Res. 35 (13), 3260–3264.

Li, W., Liao, P., Oldham, T., Jiang, Y., Pan, C., Yuan, S., Fortner, J.D., 2018. Real-time evaluation of natural organic matter deposition processes onto model environmental surfaces. Water Res. 129, 231–239.

Liao, C.-J., Lin, F.-H., Chen, K.-S., Sun, J.-S., 1999. Thermal decomposition and reconstitution of hydroxyapatite in air atmosphere. Biomaterials 20 (19), 1807–1813.

Lin, T., Chen, W., Wang, L., 2010. Particle properties in granular activated carbon filter during drinking water treatment. J. Environ. Sci. 22 (5), 681–688.

Liu, Q., Huang, S., Matinlinna, J.P., Chen, Z., Pan, H., 2013. Insight into biological apatite: physiochemical properties and preparation approaches. Biomed. Res. Int. 2013, 1–13 929748.

Maheshwari, R., 2006. Fluoride in drinking water and its removal. J. Hazard. Mater. 137 (1), 456–463.

Maity, J.P., Hsu, C.-M., Lin, T.-J., Lee, W.-C., Bhattacharya, P., Bundschuh, J., Chen, C.-Y., 2018. Removal of fluoride from water through bacterial-surfactin mediated novel hydroxyapatite nanoparticle and its efficiency assessment: adsorption isotherm, adsorption kinetic and adsorption thermodynamics. Environ. Nanotechnol. Monit. Manage 9, 18–28.

Mason, R.P., 2013. Trace Metals in Aquatic Systems. John Wiley & Sons.

Medellin-Castillo, N.A., Leyva-Ramos, R., Ocampo-Perez, R., Garcia de la Cruz, R.F., Aragon-Pina, A., Martinez-Rosales, J.M., Guerrero-Coronado, R.M., Fuentes-Rubio, L., 2007. Adsorption of fluoride from water solution on bone char. Ind. Eng. Chem. Res. 46 (26), 9205–9212.

Medellin-Castillo, N., Leyva-Ramos, R., Padilla-Ortega, E., Perez, R.O., Flores-Cano, J., Berber-Mendoza, M., 2014. Adsorption capacity of bone char for removing fluoride from water solution. Role of hydroxyapatite content, adsorption mechanism and competing anions. J. Ind. Eng. Chem. 20 (6), 4014–4021.

Meenakshi, S., Sundaram, C.S., Sukumar, R., 2008. Enhanced fluoride sorption by mechanochemically activated kaolinites. J. Hazard. Mater. 153 (1–2), 164–172.

Mendoza-Castillo, D.I., Bonilla-Petriciolet, A., Jáuregui-Rincón, J., 2015. On the importance of surface chemistry and composition of bone char for the sorption of heavy metals from aqueous solution. Desalin. Water Treat. 54 (6), 1651–1662.

Mohamed, R., Baeissa, E., 2013. Preparation and characterisation of Pd–TiO2–hydroxyapatite nanoparticles for the photocatalytic degradation of cyanide under visible light. Appl. Catal. A Gen. 464, 218–224.

Mourabet, M., El Rhilassi, A., El Boujaady, H., Bennani-Ziatni, M., El Hamri, R., Taitai, A., 2015. Removal of fluoride from aqueous solution by adsorption on hydroxyapatite (HAp) using response surface methodology. J. Saudi Chem. Soc. 19 (6), 603–615.

Nagaraj, A., Sadasivuni, K.K., Rajan, M., 2017. Investigation of lanthanum impregnated cellulose, derived from biomass, as an adsorbent for the removal of fluoride from drinking water. Carbohydr. Polym. 176, 402–410.

Nakuru Defluoridation Company Ltd http://www.cdnwaterquality.co.ke/.

Naliaka, B., 2016. Evaluation of Bone Char Defluoridation of Water using Adsorption Isotherms and the Bed Depth Service Time (BDST) Model. MSc Thesis. University of Nairobi, Nairobi, Kenia.

Näslund, J., Snell, I., 2005. GIS-Mapping of Fluoride Contaminated Groundwater in Nakuru and Baringo District, Kenya. MSc Thesis. Luleå University of Technology, Luleå, Sweden.

Nasr, A.B., Walha, K., Charcosset, C., Amar, R.B., 2011. Removal of fluoride ions using cuttlefish bones. J. Fluor. Chem. 132 (1), 57–62.

Nigri, E.M., Bhatnagar, A., Rocha, S.D.F., 2017a. Thermal regeneration process of bone char used in the fluoride removal from aqueous solution. J. Clean. Prod. 142, 3558–3570.

Nigri, E.M., Cechinel, M.A.P., Mayer, D.A., Mazur, L.P., Loureiro, J.M., Rocha, S.D., Vilar, V.J., 2017b. Cow bones char as a green sorbent for fluorides removal from aqueous solutions: batch and fixed-bed studies. Environ. Sci. Pollut. R 24 (3), 2364–2380.

Nunes-Pereira, J., Lima, R., Choudhary, G., Sharma, P., Ferdov, S., Botelho, G., Sharma, R., Lanceros-Méndez, S., 2018. Highly efficient removal of fluoride from aqueous media through polymer composite membranes. Sep. Purif. Technol. 205, 1–10.

OECD, 2018. OECD-FAO Agricultural Outlook 2018–2027.

Oladipo, A.A., Gazi, M., 2017. Application of hydroxyapatite-based nanoceramics in wastewater treatment: Synthesis, characterization, and optimization. In: Mishra, A.K. (Ed.), Sol-Gel Based Nanoceramic Materials: Preparation, Properties and Applications. Springer, pp. 231–251.

Padhi, S., Muralidharan, D., 2012. Fluoride occurrence and mobilization in geo-environment of semi-arid granite watershed in southern peninsular India. Environ. Earth Sci. 66 (2), 471–479.

Pan, J., Zheng, Y., Ding, J., Gao, C., Van der Bruggen, B., Shen, J., 2018. Fluoride removal from water by membrane capacitive deionization with monovalent anion selective membrane. Ind. Eng. Chem. Res. 57 (20), 7048–7053.

Patel, S., Han, J., Qiu, W., Gao, W., 2015. Synthesis and characterisation of mesoporous bone char obtained by pyrolysis of animal bones, for environmental application. J. Environ. Chem. Eng 3 (4), 2368–2377.

Petrone, P., Guarino, F.M., Giustino, S., Gombos, F., 2013. Ancient and recent evidence of endemic fluorosis in the Naples area. J. Geochem. Explor. 131, 14–27.

Phantumvanit, P., Songpaisan, Y., Möller, I.J., 1988. A defluoridator for individual households. Wld. Hlth. Forum 9 (4), 555–558.

Qi, Z., 2013. Proton Exchange Membrane Fuel Cells. CRC Press.

Rasool, A., Farooqi, A., Xiao, T., Ali, W., Noor, S., Abiola, O., Ali, S., Nasim, W., 2017. A review of global outlook on fluoride contamination in groundwater with prominence on the Pakistan current situation. Environ. Geochem. Health 1–17.

Raychoudhury, T., Boindala, S.P., Kalidindi, S., 2017. Performance evaluation of metal impregnated activated carbon composite for removal of fluoride under varying solution chemistry. Water Sci. Tech-W Sup. 17 (5), 1377–1385.

Reynel-Avila, H.E., Mendoza-Castillo, D.I., Bonilla-Petriciolet, A., 2016. Relevance of anionic dye properties on water decolorization performance using bone char: adsorption kinetics, isotherms and breakthrough curves. J. Mol. Liq. 219, 425–434.

Rojas-Mayorga, C., Bonilla-Petriciolet, A., Aguayo-Villarreal, I.A., Hernandez-Montoya, V., Moreno-Virgen, M., Tovar-Gómez, R., Montes-Morán, M., 2013. Optimization of pyrolysis conditions and adsorption properties of bone char for fluoride removal from water. J. Anal. Appl. Pyrolysis 104, 10–18.

Rojas-Mayorga, C.K., Silvestre-Albero, J., Aguayo-Villarreal, I.A., Mendoza-Castillo, D.I., Bonilla-Petriciolet, A., 2015a. A new synthesis route for bone chars using CO2 atmosphere and their application as fluoride adsorbents. Micropo. Mesopo. Mater. 209, 38–44.

Rojas-Mayorga, C.K., Bonilla-Petriciolet, A., Silvestre-Albero, J., Aguayo-Villarreal, I.A., Mendoza-Castillo, D.I., 2015b. Physico-chemical characterization of metal-doped bone chars and their adsorption behavior for water defluoridation. Appl. Surf. Sci. 355, 748–760.

Rojas-Mayorga, C.K., Bonilla-Petriciolet, A., Sánchez-Ruiz, F.J., Moreno-Pérez, J., Reynel-Ávila, H.E., Aguayo-Villarreal, I., Mendoza-Castillo, D., 2015c. Breakthrough curve modeling of liquid-phase adsorption of fluoride ions on aluminum-doped bone char using micro-columns: effectiveness of data fitting approaches. J. Mol. Liq. 208, 114–121.

Rostamia, I., Mahvib, A.H., Dehghanib, M.H., Baghania, A.N., Marandid, R., 2017. Application of nano aluminum oxide and multi-walled carbon nanotube in fluoride removal. Desalin. Water Treat. 1, 1–6.

Roy, S., 2018. Synthesis of graphene oxide using tea-waste biochar as green substitute of graphite and its application in de-fluoridation of contaminated water. Am. J. Chem. Res. 1, 1–19.

Ruthven, D.M., 2008. Fundamentals of adsorption equilibrium and kinetics in microporous solids. In: Karge, H.G., Weitkamp, J. (Eds.), Adsorption and Diffusion. Springer, Berlin, Heidelberg, pp. 1–43.

Sani, T., Gómez-Hortigüela, L., Pérez-Pariente, J., Chebude, Y., Díaz, I., 2016. Defluoridation performance of nano-hydroxyapatite/stilbite composite compared with bone char. Sep. Purif. Technol. 157, 241–248.

Skinner, H., Jahren, A., 2004. Biomineralization 8.04. In: Treatise on Geochemistry. vol. 6. pp. 182–216.

Smittakorn, S., Jirawongboonrod, N., Mongkolnchai-Arunya, S., Durnford, D., 2010. Homemade bone charcoal adsorbent for defluoridation of groundwater in Thailand. J. Water Health 8 (4), 826–836.

Soni, C., Wang, Z., Dalai, A., Pugsley, T., Fonstad, T., 2009. Hydrogen production via gasification of meat and bone meal in two-stage fixed bed reactor system. Fuel 88 (5), 920–925.

Soni, C.G., Dalai, A.K., Pugsley, T., Fonstad, T., 2011. Steam gasification of meat and bone meal in a two-stage fixed-bed reactor system. Asia Pac. J. Chem. Eng. 6 (1), 71–77.

State of South Carolina Department of Health and Environmental Control Water Supply Division, 1980. Fluoride Reduction in Community Water Supplies.

Sternitzke, V., Kaegi, R., Audinot, J.-N., Lewin, E., Hering, J.G., Johnson, C.A., 2012. Uptake of fluoride from aqueous solution on nano-sized hydroxyapatite: examination of a fluoridated surface layer. Environ. Sci. Technol. 46 (2), 802–809.

Tchomgui-Kamga, E., Alonzo, V., Nanseu-Njiki, C.P., Audebrand, N., Ngameni, E., Darchen, A., 2010. Preparation and characterization of charcoals that contain dispersed aluminum oxide as adsorbents for removal of fluoride from drinking water. Carbon 48 (2), 333–343.

Terasaka, S., Kamitakahara, M., Yokoi, T., Ioku, K., 2014. Effect of preparation temperature on the ability of bone char to remove fluoride ion and organic contaminants. J. Ceram. Soc. Japan. 122 (1432), 995–999.

Thanh, D.N., Novák, P., Vejpravova, J., Vu, H.N., Lederer, J., Munshi, T., 2017. Removal of copper and nickel from water using nanocomposite of magnetic hydroxyapatite nanorods. J. Magn. Magn. Mater. 456, 451–460.

Thoelke, J.B., 1993. Magnetization and Magnetostriction in Highly Magnetostrictive Materials. MSc Thesis. Iowa State University, Ames, Iowa.

Tovar-Gómez, R., Moreno-Virgen, M., Dena-Aguilar, J., Hernández-Montoya, V., Bonilla-Petriciolet, A., Montes-Morán, M., 2013. Modeling of fixed-bed adsorption of fluoride on bone char using a hybrid neural network approach. Chem. Eng. J. 228, 1098–1109.

Tripathy, S.S., Bersillon, J.-L., Gopal, K., 2006. Removal of fluoride from drinking water by adsorption onto alum-impregnated activated alumina. Sep. Purif. Technol. 50 (3), 310–317.

Usón, A.A., López-Sabirón, A.M., Ferreira, G., Sastresa, E.L., 2013. Uses of alternative fuels and raw materials in the cement industry as sustainable waste management options. Renew. Sust. Energ. Rev. 23, 242–260.

Waghmare, S., Arfin, T., Rayalu, S., Lataye, D., Dubey, S., Tiwari, S., 2015. Adsorption behavior of modified zeolite as novel adsorbents for fluoride removal from drinking water: surface phenomena, kinetics and thermodynamics studies‖. IJRRSET 4 (12), 4114–4124.

Wang, X.-H., Song, R.-H., Yang, H.-C., Shi, Y.-J., Dang, G.-B., Yang, S., Zhao, Y., Sun, X.-F., Wang, S.-G., 2013. Fluoride adsorption on carboxylated aerobic granules containing Ce (III). Bioresour. Technol. 127, 106–111.

Wang, J., Chen, N., Li, M., Feng, C., 2018. Efficient removal of fluoride using polypyrrole-modified biochar derived from slow pyrolysis of pomelo peel: sorption capacity and mechanism. J. Polym. Environ. 26 (4), 1559–1572.

Warren, G., Robinson, J., Someus, E., 2009. Dissolution of phosphorus from animal bone char in 12 soils. Nutr. Cycl. Agroecosys. 84 (2), 167–178.

Wei, F., Cao, C., Huang, P., Song, W., 2015. A new ion exchange adsorption mechanism between carbonate groups and fluoride ions of basic aluminum carbonate nanospheres. RSC Adv. 5 (17), 13256–13260.

Xie, J., Meng, X., Zhou, Z., Li, P., Yao, L., Bian, L., Gao, X., Wei, Y., 2013. Preparation of titania/hydroxyapatite (TiO2/HAp) composite photocatalyst with mosaic structure for degradation of pentachlorophenol. Mater. Lett. 110, 57–60.

Yami, T.L., Du, J., Brunson, L.R., Chamberlain, J.F., Sabatini, D.A., Butler, E.C., 2015. Life cycle assessment of adsorbents for fluoride removal from drinking water in East Africa. Int. J. Life Cycle Assess. 20 (9), 1277–1286.

Ye, Y., Yang, J., Jiang, W., Kang, J., Hu, Y., Ngo, H.H., Guo, W., Liu, Y., 2018. Fluoride removal from water using a magnesia-pullulan composite in a continuous fixed-bed column. J. Environ. Manag. 206, 929–937.

Zhang, Y.-X., Jia, Y., 2018. Fluoride adsorption on manganese carbonate: ion-exchange based on the surface carbonate-like groups and hydroxyl groups. J. Colloid. Interf. Sci. 510, 407–417.

Zhu, J., Zhao, H., Ni, J., 2007. Fluoride distribution in electrocoagulation defluoridation process. Sep. Purif. Technol. 56, 184–191.

Zhu, H., Wang, H., Wang, G., Zhang, K., 2011. Removal of fluorine from water by the aluminum-modified bone char. In: 2010 International Conference on Biology, Environment and Chemistry IPCBEE. vol.1. IACSIT Press, Singapore, pp. 455–457.

Zhu, P., Cao, Z., Ye, Y., Qian, G., Lu, B., Zhou, M., Zhou, J., 2013. Reuse of hazardous calcium fluoride sludge from the integrated circuit industry. Waste Manag. Res. 31 (11), 1154–1159.

Zúñiga-Muro, N., Bonilla-Petriciolet, A., Mendoza-Castillo, D., Reynel-Ávila, H., Tapia-Picazo, J., 2017. Fluoride adsorption properties of cerium-containing bone char. J. Fluor. Chem. 197, 63–73.